D-Shaped optical fiber sensor via evanescent wave effect

Master's Thesis of

Sarah Pulikottil Alex, 2399500

At Technical University of Vienna

Reviewer: Prof. Dr.-Ing. Christoph Stiller
Advisor: Dr. Ignác Bugár

April 04, 2022 – October 04, 2022

Karlsruhe School of Optics and Photonics
Schlossplatz 19
76131 Karlsruhe

I herewith declare that the present thesis is original work written by me alone, that I have indicated completely and precisely all aids used as well as all citations, whether changed or unchanged, of other theses and publications, and that I have observed the KIT Statutes for Upholding Good Scientific Practice, as amended.

Wien, 04/10/2022

. . . . . .

(Sarah Pulikottil Alex, **2399500**)

Ich versichere wahrheitsgemäß, die Arbeit selbstständig verfasst, alle benutzten Hilfsmittel vollständig und genau angegeben und alles kenntlich gemacht zu haben, was aus Arbeiten anderer unverändert oder mit Abänderungen entnommen wurde sowie die Satzung des KIT zur Sicherung guter wissenschaftlicher Praxis in der jeweils gültigen Fassung beachtet zu haben.

Wien, 04/10/2022

. . . . . .

(Sarah Pulikottil Alex, **2399500**)

ABSTRACT

Optical fibers are used for sensing applications by continuously monitoring the changes in physical, chemical and biological parameters. Fiber optic sensors (FOS) provide the possibility to measure various parameters like temperature, strain, liquid sensing with simple sensor design. The sensing information is transferred by optical sensors through modulation in intensity, phase, polarization. Optical fiber sensors have advantages compared to conventional sensors due to absence of electromagnetic interference, ability to sense in harsh environmental condition and remote sensing. This class of sensors are widely usable due to various simple sensor designs and measurement techniques available which improves the sensing capability of the sensor.

The aim of this master thesis is to explore new areas of evanescent wave effect-based fiber sensor using a specialty optical fiber. A novel D-shaped optical fiber is developed with homogenous asymmetric cross-section along its whole length. This type of fiber is utilized throughout the course of the thesis to enhance the evanescent wave effect for sensing. Different geometrical configurations of the optical fiber are utilized to study the improvement in the sensing performance. Refractive index sensing of liquids is the major focus of the experimental work. Isopropanol and distilled water are the optical media under test for liquid sensing . A D-shaped fiber with a length of 20 cm is utilized with 4-cm long uncoated region in the central part of the fiber acting as the sensing region. The asymmetrically positioned thin cladding enhances interaction of evanescent field with the external environment. The sensing performance expressed polarization dependence with vertical polarization being prone to more losses due to the enhanced evanescent wave effect

Spectral measurements revealed significant changes by varying the physical parameter: refractive index. Sensing liquids like distilled water and isopropanol helps to quantify the content of such kinds of compound in their mixture. Distilled water, being a non-reactive and miscible liquid in most chemicals, can easily be a source of contamination in isopropanol. A simple approach based on D-shaped fiber sensing provides a method to measure such contamination by studying the spectral intensity changes at different proportions of the two liquids in a mixture. The evanescent wave interaction and hence the sensitivity of FOS is further improved by the implementation of U-bend geometry. U-bend geometry offers higher sensitivity due to mode displacement that occurs with the bending of the fiber. The ambition of the work is to offer new approaches for fiber-based sensing of materials that are industrially important.

Keywords: Fiber optic sensor, Evanescent wave effect, D-shaped fiber

ABSTRACT

Optische Fasern werden für Sensoranwendungen eingesetzt, indem sie die Veränderungen physikalischer, chemischer und biologischer Parameter kontinuierlich überwachen. Faseroptische Sensoren (FOS) bieten die Möglichkeit, verschiedene Parameter wie Temperatur, Dehnung und Flüssigkeit mit einem einfachen Sensordesign zu messen. Die Messinformationen werden von optischen Sensoren durch Modulation der Intensität, Phase und Polarisation übertragen. Faseroptische Sensoren haben gegenüber konventionellen Sensoren den Vorteil, dass keine elektromagnetischen Störungen auftreten, dass sie auch unter rauen Umgebungsbedingungen messen können und dass sie ferngesteuert werden können. Diese Klasse von Sensoren ist aufgrund verschiedener einfacher Sensordesigns und Messverfahren, die die Erfassungsfähigkeit des Sensors verbessern, weit verbreitet.

Das Ziel dieser Masterarbeit ist die Erforschung neuer Bereiche der auf dem Evaneszenzwelleneffekt basierenden Fasersensoren unter Verwendung einer speziellen optischen Faser. Es wird eine neuartige D-förmige optische Faser mit homogenem asymmetrischem Querschnitt über die gesamte Länge entwickelt. Dieser Fasertyp wird im Verlauf der Arbeit verwendet, um den Evaneszenzwelleneffekt für die Sensorik zu verstärken. Es werden verschiedene geometrische Konfigurationen der optischen Faser verwendet, um die Verbesserung der Erfassungsleistung zu untersuchen. Die Messung des Brechungsindex von Flüssigkeiten steht im Mittelpunkt der experimentellen Arbeit. Isopropanol und destilliertes Wasser sind die zu prüfenden optischen Medien für die Flüssigkeitssensorik. Es wird eine D-förmige Faser mit einer Länge von 20 cm verwendet, wobei ein 4 cm langer unbeschichteter Bereich im zentralen Teil der Faser als Sensorbereich dient. Der asymmetrisch angeordnete dünne Mantel verstärkt die Wechselwirkung des evaneszenten Feldes mit der äußeren Umgebung. Die Erfassungsleistung war polarisationsabhängig, wobei die vertikale Polarisation aufgrund des verstärkten Effekts der evaneszenten Wellen zu größeren Verlusten führte.

Spektrale Messungen ergaben signifikante Veränderungen durch die Variation des physikalischen Parameters: des Brechungsindexes. Die Messung von Flüssigkeiten wie destilliertem Wasser und Isopropanol hilft bei der Quantifizierung des Gehalts dieser Arten von Verbindungen in ihrem Gemisch. Da destilliertes Wasser eine nicht reaktive und mit den meisten Chemikalien mischbare Flüssigkeit ist, kann es in Isopropanol leicht zu einer Verunreinigung kommen. Ein einfaches Verfahren auf der Grundlage von D-förmigen Fasern bietet eine Methode zur Messung solcher Verunreinigungen, indem die Änderungen der spektralen Intensität bei unterschiedlichen Anteilen der beiden Flüssigkeiten in einer Mischung untersucht werden. Die Wechselwirkung mit evaneszenten Wellen und damit die Empfindlichkeit von FOS wird durch die Implementierung einer U-förmigen Geometrie weiter verbessert. Die U-Bogen-Geometrie bietet eine höhere Empfindlichkeit aufgrund der Modenverschiebung, die durch die Biegung der Faser entsteht. Das Ziel dieser Arbeit ist es, neue Ansätze für die faserbasierte Messung von industriell wichtigen Materialien zu bieten.

Schlüsselwörter: Faseroptischer Sensor, Evaneszenzwelleneffekt, D-förmige Faser

PREFACE

Carrying out my Master's Thesis work at, "Technical University, Vienna" has been a journey of great learning experience. I would like to express my gratitude to the management of Photonics Institute at TU, Vienna for giving me this opportunity. It has been a privilege to be given the exposure to various state of the art technical facilities in the labs and my Master's Thesis would have not been completed without the guidance and assistance of quiet a few people.

Foremost, I thank Prof. Dr. Andrius Baltuška for giving me a chance to work in his group for my Master Thesis and for all his support and constant encouragement.

I would like to express my sincere gratitude to my Project Supervisor, Dr. Ignác Bugár for helping and guiding me to accomplish this work. I would like to acknowledge and thank him for suggesting the topic for my study and educating me with nuances of the subject both at work bench and with theoretical insights. He has been a great source of inspiration and support all through this work and especially when the going became tough.

I am also thankful to Prof. Dr. Ing. Christoph Stiller for being my guide and Julian Truetsch for his timely advice on project technicalities and guiding me through the course of this project. Without his unstinted support it would have been difficult for me to complete this work in the stipulate time.

Last but not the least, I profoundly acknowledge the benevolent financial support provided by Erasmus Mundus & Europhotonics team to pursue this program. I also place on record my sincere thanks to all my teachers and mentors at Aix Marseille University, KIT, and Tampere University where I had the opportunity to study the fascinating subject of photonics.

Vienna, 04 October 2022

Sarah Pulikottil Alex

CONTENTS

LIST OF FIGURES

LIST OF SYMBOLS AND ABBREVIATIONS

CW	Continuous-wave
EMI	Electromagnetic interference
EWA	Evanescent wave absorption
FOS	Fiber optic sensor
IPA	Isopropyl alcohol
IR	Infrared
NA	Numerical aperture
NIR	Near infrared region
LED	Light emitting diode
LP	Linearly polarized
RI	Refractive index
SEM	Scanning electron microscope
SPR	Surface plasma resonance
TIR	Total internal reflection
TE	Transverse electric
TFBG	Tilted fiber Bragg grating
TM	Transverse magnetic
UV	Ultraviolet

1. INTRODUCTION

Fiber optic sensors (FOS) are a class of sensors that are used in various applications ranging from structural health monitoring [1], biosensing [2] and chemical sensing [3]. FOS are widely used in the real time monitoring of various analytes with different approaches to improve the sensing performance. FOS are widely acceptable due to their small size, light weight, resistance against harsh conditions, low electromagnetic interference (EMI). This makes FOS usable in any kind of environment and still provide efficient sensing. Their non-conductive and non-corrosive behavior also makes them suitable for various industrial applications that are not possible using conventional sensors. This makes optical sensors far more convenient than their electrical counterparts (thermocouples, strain gauges) which can be proven as inefficient in certain conditions. Different FOS techniques can be implemented depending on the applications and the parameters sensed. Starting from 1960s the usage of FOS in the medical industry became one of the major approaches [4] due to their inert nature, immunity to EMI and non-invasiveness by removing physical contact with the organs and tissues. Also, information from the human body can be accessed using fiber optic sensors in multiple fiber bundles as a single probe.

Chemical sensing is being researched extensively in various industries including for monitoring the environment, examination of organic liquids, medicine and chemical analysis [5]. Fiber based sensors have gained attention in chemical sensing due to their ability of remote measurement and system compactness. FOS can be either intrinsic or extrinsic. Refractive index-based sensors are demonstrated using various approaches. Conventional refractive index (RI) sensors includes interferometric sensors technology [6], [7] (like Fabry-Perot, Mach Zehnder) which measures small changes in RI, intrinsic methods using photonic crystal fibers [8], fiber Bragg grating [9] etc. Evanescent wave-based sensing which is a recently progressed sensing design, falls under the extrinsic sensor category for chemical sensing [10]. It allows simpler fabrication method compared to other RI sensors with high efficiency and robustness. Evanescent wave sensing can be based either on RI sensing or evanescent absorption- based sensor (EWA). Other design characteristics also plays an important role in controlling and establishing the

sensing capability. In particular, fiber core diameter, length of fiber, and fiber probe geometry are important parameters for the design of such sensors [11]. Moreover, various geometrical approaches have been proposed to enhance sensing capability as tapering, etching, U-bend. For liquid sensing, it is important to understand the RI or absorbance of liquids to find out the wavelength at which maximum signal change occurs. Evanescent wave effect enhances with increasing wavelength [11]. For example, it was noticed that in the infrared region, there is higher RI and absorbance for certain liquids [11].

The main aim of the thesis is to demonstrate RI sensing based on the evanescent wave effect. This is accomplished using a D-shaped optical fiber such that the flat surface of D-shaped fiber is exposed to the interaction between evanescent wave and external environment. RI sensing is demonstrated where the evanescent wave interacts with the liquid under test. Distilled water and isopropanol, which are common and industrially relevant liquids are used to demonstrate RI sensing. Detection of liquids that are commercially and industrially important solvents with low-cost and easily fabricated sensor system provides an added advantage. Geometrical configuration of the fiber and other design parameters (e,g. Straight fiber geometry U-bend geometry, tapered fiber) are described to establish and investigate the sensing capability of D-shaped fiber. Sensing performance was monitored by spectral measurements where the change in spectral characteristics was evaluated to understand the sensing performance. Sensing performance can be depicted in terms of spectral changes that occurs after the optical signal interacts with the external medium. The changes in spectrum due to liquid detection were examined to study the stability, reliability and repeatability of the sensor.

The rest of the thesis is organized as follows. *Chapter 2* describes the theoretical background about the principles of light propagation through the fiber, evanescent wave sensing and related useful parameters. The geometrical configuration involved in improving the sensitivity of the sensor will also be discussed. These are needed to understand the light interaction with the external environment for sensing and help interpret the experimental results. *Chapter 3* focuses on the methodology and experimental work carried out to design the sensor system. The results obtained from sensing experiment is discussed in detail in Chapter 4 which ensures the validation of sensor design for future applications. Finally, Chapter 5 gives an outlook and insight of the thesis in the conclusion.

2. THEORETICAL BACKGROUND

This chapter presents the fundamental concepts that are useful to understand the working principle of evanescent wave-based fiber optic sensor. The chapter starts with the basics of light propagation through optical fiber, followed by discussion of evanescent wave sensor and a brief description on femtosecond laser.

2.1 Light propagation along an optical fiber

Optical fiber [12] is a dielectric waveguide with circular symmetry of its cross section enabling the transmission optical fields to large distances with a relatively low loss. Standardly it consists of a circular central core surrounded by cladding. The core has a higher RI than the cladding, which allows optical field propagation along the fiber based on the phenomenon called total internal reflection (TIR). The principle of TIR originates from the ray theory and it can occur when the light propagates from a medium of high RI (n_1) to a medium of low RI (n_2). In this case, if the incident angle is greater than the critical angle (θ_c), the rays are reflected totally back to the medium of high RI. Thus, TIR enables field preservation and low loss propagation in the high refractive index core of the fiber, when it is illuminated in an accurate way. The common fiber material is fused silica [13], which is doped by other oxides in the core area to increase the RI in that region. The simplest fiber structure, called step-index fiber, has two discrete RI levels: n_1 and n_2 devoted to the core and cladding respectively. However, besides the core and cladding of the optical fiber, mostly it has around the cladding an outer layer called coating, made of acrylate, which acts as a non-optical media protecting the glass-made part of the waveguide.

There are two types of rays propagating through the optical fiber: meridional and skew rays [14]. Meridional rays regularly cross the propagation axis of the fiber and they ensure the transmission of the major part of the optical power. Whereas, skew rays propagate without passing through the axis of optical fiber because they are confined close to the boundary of the core. ***Figure 2.1*** depicts a typical scenario of meridional and skews rays imping and propagating in an optical fiber. In sensing applications, only meridional rays are considered for analysis and simplicity. Ray theory provides acceptable predictions for fiber dimensions much larger than wavelength of light. Thus, it cannot be used in the case of dimensions comparable to the applied wavelength. Also, certain intricacies of the propagation character cannot be demonstrated using ray theory. Importantly, the

dominance of some discrete transversal modes and their effect beyond the fiber core is not explained with the ray theory. The description and evaluation of such aspects require the consideration of the wave theory of the optical field.

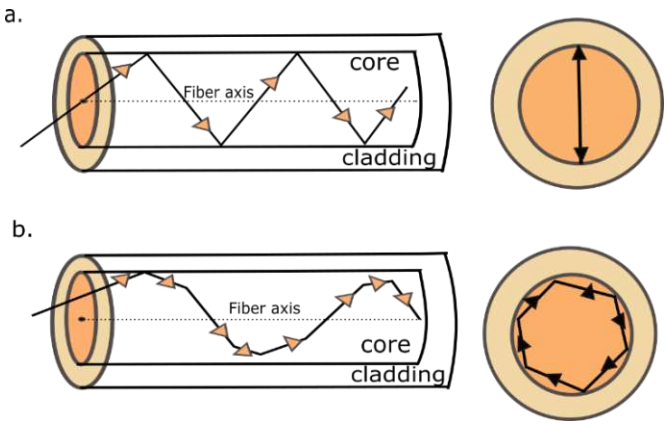

Figure 2.1. *Propagation of a light ray along an optical fiber a). Meridional rays cross the fiber axis. b). Skew rays do not cross the fiber axis but propagate close to the core-cladding boundary.*

2.1.1 Wave theory

The wave theory explains the propagation of optical radiation based on electromagnetic wave behavior. The elementary unit of such a description is a plane wave, which means wavefront perpendicular to the direction of propagation with identical phase in the whole plane. However, in the fiber more complex waveforms are formed and all of them express deterministic transversal intensity patterns depending on the character of the incident EM field. Certain intensity patterns are preserved along the whole fiber length as superposition of multiple plane waves. When a part of the plane wave undergoes a shift in phase due to reflection, it interferes with its other parts thereby resulting in destructive or constructive effect. Thus, only the intensity patterns, which are outcomes of such constructively interference will be preserved and propagate along the fiber. Each intensity field pattern, termed as modes has a different profile, different effective RI and propagation constant, determining its propagation velocity. Also, the mode structure of the fiber and their mentioned characteristics depend on the wavelength of the incident field.

In the case of propagation along an optical fiber, there cannot be both electric and magnetic field vectors that are perpendicular to the direction of propagation. Therefore, standardly the modes are classified under the assumption that the electric field vector fulfills this condition and termed as TE modes. When the fiber is assumed to be weakly guiding, the modes propagating through them are termed as linearly polarized (LP) modes. In case of stronger guidance, either the transverse electric (TE) or transverse magnetic

(TM) modes propagate. The various field patterns correspond to orders of the mode. The order depends on the number of intensity maxima in the field pattern of fiber core. For example, there is one field maxima for the TE_0 which is the fundamental mode. The order of modes increases with the increase in the number of field maxima. ***Figure 2.2*** shows the various modes propagating through the fiber. For a given n_2 and n_1 and wavelength λ, the number of modes become smaller if the core radius is decreased. Also, fibers with low numerical aperture (NA) have less modes propagating inside the fiber.

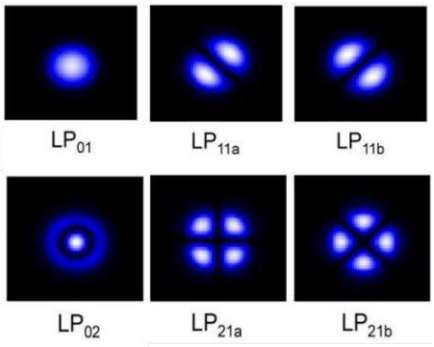

Figure 2.2 *Transversal intensity patterns of the lower modes propagating inside the fiber (adapted from [15]).*

Modes that can propagate at a shorter wavelength may be not guided in the fiber at longer wavelengths. Some modes are not available at a fixed wavelength i.e., there is a highest order mode limit for each particular wavelength. Similarly, beyond a limiting long wavelength only one mode is guided in the fiber. This mode is termed as the fundamental mode of the fiber. Wavelength that can accommodate only the fundamental mode and not any other further modes is known as the cutoff wavelength. Thus, based on the mode structure of the fiber at a given wavelength, it is classified as single or multi-mode. In the following section, the basic mathematical relations will be presented, which characterize the mode structure of the fiber in the case of a step-index fiber type at known structure parameters.

2.2 Basic parameters of optical fibers

Numerical aperture: NA is defined as the sine function of the maximum incidence angle of ray, which the fiber can possess to obey TIR. The NA defines the range of acceptable angles allowing propagation through the fiber at reduced losses. Angles beyond the NA will lead to propagation with significant radiative losses. The NA can be expressed via RI as shown by *equation* (***2.1)***

$$NA = sin\,\emptyset = \sqrt{n_1^2 - n_2^2} \tag{2.1}$$

where n_1 and n_2 are the core and cladding RI, $\emptyset$ is the half acceptance angle [14].

V parameter: It is also termed as normalized optical frequency which helps to determine the number of the modes guided by the fiber. It is a dimensionless quantity. It depends on the wavelength of light in air*(λ)*, core radius *(a)*, and the numerical aperture *(NA)* of the fiber as expressed by *equation (**2.2**)*.

$$V = \frac{2\pi}{\lambda}\, aNA = \frac{2\pi}{\lambda}\, a\sqrt{n_1^2 - n_2^2} \tag{2.2}$$

The number of modes in a step-index multimode fiber is estimated by $M \approx \frac{V^2}{2}$ which is usable for high *V* parameter values. For a single-mode operation, the V parameter should be less than 2.405.

Cutoff wavelength: It is the shortest *λ* at which the fiber acts like a single-mode waveguide. At even shorter wavelengths more than one mode is guided by the fiber. As the wavelength increases, the modes propagating through it reduces as seen in *equation (**2.3**)*.

$$\lambda_c = \frac{2\pi}{V_c} a\sqrt{n_1^2 - n_2^2} \tag{2.3}$$

where *a* is the core radius of fiber, n_1 and n_2 are the core and cladding RI respectively, λ_c is the cutoff wavelength and V_c is the cutoff *V* parameter (2.405).

Above a certain wavelength, only the fundamental mode can traverse through the fiber and this wavelength is termed in as the cutoff wavelength. In this case only the LP_0 modes can propagate through the core. Whereas, below the cutoff wavelength also higher-order modes like LP_{11} can propagate.

There are two types of fiber based on the mode structures propagating through it: single mode fiber and multi-mode fiber. Single-mode fiber guides only the fundamental mode. The core is small with core diameter around 8-10 μm in the case of standard telecom fibers designed for the wavelength of 1560 nm [14] . The normalized frequency or the *V* number for a single-mode fiber is less than or equal to 2.405. When the value of V parameter is higher, the power fraction propagating in the cladding exceeds 10%. Usually, single mode fiber has a relatively low loss and high transmission capability.

Multimode fiber, as the name suggests, is a type of fiber that allows large number of modes to propagate inside the fiber at a given wavelength. NA and core size are the main parameters that affects the normalized frequency and therefore the number of modes as seen in *equation* (***2.2***). Higher number of modes propagate through the fiber with increasing values of NA and core size. The core size of a strongly multimode fiber is typically 50-100 µm and the NA is 0.20-0.29 [14]. Such values of the basic parameters support efficient in-coupling of the optical radiation. On the other hand, the multimode fibers exhibit enhanced dispersion effect. The multimode fiber undergoes intermodal dispersion because different modes express different propagation constants.

2.3 Factors affecting fiber optic transmission

Transmission of light through optical fiber is an aspect to be discussed while introducing the working principle of fiber optic sensors. The propagation of light is affected due to various factors including attenuation, dispersion etc. It is necessary to analyze the effect of such factors in area of optical sensor development and application.

2.3.1 Attenuation

Attenuation is about the loss of optical signal that arises due to physical properties of fiber which reduce the power of the initial signal. Attenuation of optical signal through fiber is given by *equation* (***2.4***)

$$\alpha = \frac{10}{L} log_{10} \frac{P_i}{P_o} \tag{2.4}$$

where α is the attenuation through the fiber, L is the length of the fiber, P_i the initial power at the input of the fiber and P_o is the output power at the end of propagation through fiber. Attenuation in fibers is dependent on wavelength, fiber structural properties and on the material with which the fiber is fabricated. Loss of power occurs due to various physical phenomena and some of them are described as follows.

Absorption: Attenuation through fiber can take place due to absorption of light in the fiber material. Absorption occurs when optical signal is absorbed by some intrinsic or extrinsic material feature leading to loss of power at the output end of fiber. It is one of the main causes of losses in the optical fiber. Some of the reasons that can lead to reduction in optical power are related to fiber's material properties or its atomic structure. Absorption can also occur due to impurities present in the fiber or any external material which absorbs the light energy [14]. Based on this, absorption can further be classified into two types: intrinsic and extrinsic absorption.

Intrinsic absorption occurs due to the presence of small changes in the fiber material properties which cannot be avoided during manufacturing of glass. Silica fiber has low intrinsic absorption compared to other fiber materials which makes it suitable for reduced absorption effect. The absorption in the infrared wavelength occurs due to vibration of atomic bonds. The electromagnetic field of the optical signal interacts with the vibration frequency of silicon - oxygen bonds transferring light energy and causing absorption [14]. Extrinsic absorption occurs due to impurities or defects present in the material. This includes metal impurities or even presence of OH^- bond due to traces of water in silica glasses [14]. Such bonds have a fundamental absorption at a wavelength of 2700 nm [14]. Thus, it is important to reduce the traces of water impurities in the fiber to avoid absorption.

Scattering: Attenuation of optical signal can also be caused through elastic scattering of light. Scattering occurs due to changes in the material density throughout the fiber. The density changes arise due to dopants or structural defects present in glass that was formed during the manufacturing of glass material or the fiber itself. When the optical signal propagates through the fiber, it scatters light in all direction due to density changes in the material. Elastic scattering basically occurs in two types known as the Rayleigh scattering and Mie scattering.

Rayleigh scattering takes place when the density fluctuations present in the material have sub-microscopic dimensions. This is one of the major loss mechanisms that occurs for the wavelength range of 700 nm to 1600 nm for commercial fibers [14]. This type of scattering occurs when the fluctuations size is less than one-tenth of wavelength of source being used. It is also known that Rayleigh scattering is inversely proportional to fourth power of wavelength $(1/\lambda^4)$. Thus, longer wavelengths show significantly lower Rayleigh scattering effects than shorter wavelengths.

On the other hand, Mie scattering occurs when the fiber defects are larger in size. When the size of fluctuations exceeds one-tenth of the wavelength of source then the scattering mechanism is governed by Mie scattering. The scattering occurs also outside of the core region due to defects of larger size.

Bending loss: Bending of the fiber can also reduce the optical power propagating in the fiber core. Fiber bend can transfer the modes from the core more towards the cladding reducing the modes propagating in the core. When the bend radius exceeds a critical limit (or radius at which the losses increase exponentially), there are higher losses due to optical power radiated out of the fiber core in the form of higher-order modes. Bending loss can be reduced by decreasing the sensitivity of fiber. This can be either achieved

by increasing the RI of core and also by increasing the overall diameter of fiber [14]. Bending losses are also dependent to some extent on wavelength of light being used. Longer wavelength tends to have higher losses mostly when it propagates through single-mode fiber. Apart from the macro bending losses, micro bending losses can take place when micro bends are present in the fiber. This type of bending loss emerges due to geometrical defects in the fiber fabrication.

2.3.2 Dispersion

Dispersion of light can be explained as the spreading of optical signal in time when propagating along the optical fiber. There are two types of dispersion, intermodal and intramodal. Intermodal dispersion occurs mainly in multimode fibers where large NA allows different modes to guide through the fiber at different angles. This makes the modes to traverse different path lengths at the same span of time leading to spreading of the pulse in time. The increase of the fiber length can lead to enhancement of intermodal dispersion. Whereas, intermodal dispersion is not relevant in single-mode fiber due to only the fundamental mode propagating through the fiber.

Intramodal dispersion mainly occurs in single mode fiber where it mainly consists of two major types called the material dispersion and waveguide dispersion. Material dispersion arises due to the dependence of RI on the wavelength. All laser sources have a finite bandwidth and this range of laser wavelengths propagate with different speed in the fiber and exit the fiber at different times leading to broadening of an input pulse [16]. At longer wavelengths, material dispersion is weaker.

Waveguide dispersion is caused by the structure of waveguide, which is considered mostly in single mode fiber, because it is even weaker than the intermodal dispersion. Optical signal in the cladding expresses higher velocity due to lower RI of the cladding in comparison to RI of core causing broadening of the pulse. The broadening of pulse due to chromatic dispersion is the combined effect of material and waveguide dispersion. The linewidth of source plays an important role for this type of dispersion in addition to V parameter, fiber core size and wavelength of light source [16]. Waveguide dispersion in multimode fiber is negligible compared to material dispersion due to higher core size and weaker cladding effect on the propagation.

2.3.3 Laser beam diameter

Beam diameter is a key factor to be analyzed in the case of fiber optic sensing. It is necessary to check if the whole laser beam is in-coupled to the fiber without any portion

being clipped. The beam diameter should be about 2/3 portion of core diameter of fiber in order to ensure optimal coupling into the fiber. In general, a lens is used to focus the beam to express such beam size in the focal plane. Thus, it is important to use lens with appropriate focal length taking into consideration also the wavelength of the laser source. We can calculate beam diameter in the focal plane using *equation* (***2.5***).

$$2w_o = \frac{4M^2\lambda f}{\pi D} \tag{2.5}$$

where w_o is the beam radius, M^2 is the beam quality factor, λ is the wavelength of light, f is the focal length of lens and D is the diameter of beam at the lens.

The beam diameter or spot size is defined as transversal distance at which the irradiance is $1/e^2$ times fraction of the irradiance at the center of the beam. In order to ensure effective in-coupling, the lens diameter should be at least two times the value of beam diameter in order to avoid the clipping of a Gaussian beam [17]. It is also better to have a lens that does not have strong aberrations. The last parameter is the M^2 which is the beam quality factor determining the quality of laser beam. It gives the ratio of divergence of a real beam to the divergence of ideal (diffraction-limited) beam which has a Gaussian profile and the smallest possible waist radius [18].

2.4 Fiber optic sensing

Optical fibers were developed and utilized initially for communication purposes. Later, fiber optics emerged among others as a promising tool for sensing applications. There has been massive advancement of the fiber optics sector during the last decades leading to increased production of optical fibers. The utilization of FOS has exponentially increased due to its advantages. It involves aspects like remote sensing and application in harsh environment conditions like high temperature, or highly corrosive environment [4]. The other important advantages are its electrical passiveness and small size, light weight and compactness which makes it useable without any external factors. Fibers are immune to EMI and provides higher sensitivity and resolution which leads to better sensing performance [4]. Thus, FOS are preferred over electronic devices which led to increasing demand of FOS in various applications from military to medical industry. Wide range of physical properties such as temperature, strain, humidity, pressure and also chemical sensing are applicable using optical fibers [4].

Possible parameters of optical signal that affect the sensor performance are the change in intensity, amplitude in the spectrum or the signal power, phase and polarization conditions. The FOS system consists of various components which together makes it a usable device as shown in ***Figure 2.3.*** It includes an optical source (e.g LED or laser), optical fiber which can be either single-mode or multi-mode, a transducer which converts a physical quantity to signal, a signal detector and finally a circuitry which can process the optical signal to obtain data in feasible form.

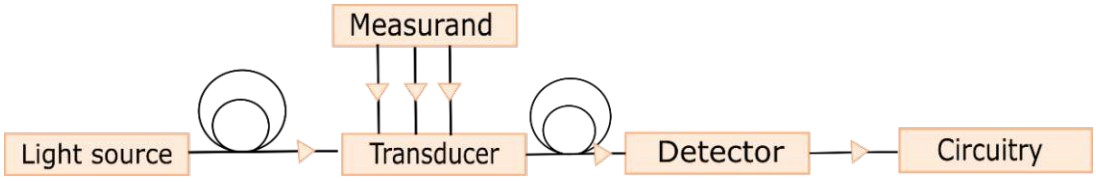

Figure 2.3. *Structure of FOS (adapted from **[4]**)*

Fiber optic sensors can be classified based on the modulation caused in the optical signal. The following parameters that influence the signal are

Modulation of Intensity: Change in physical quantities such as strain, temperature can be depicted as function of intensity variation in sensing experiments. The changes in intensity can be measured at the operating wavelength as transmission, absorption, reflection or even with micro bending [4]. Dependence on polarization orientation can also be analyzed using modulation of intensity. Intensity monitoring can be utilized for studying the perturbation of a physical quantity which is a direct measure of sensing effect. It is important to have high illumination available for intensity modulated sensor than for phase modulated sensor [4].

Modulation of phase: Phase of the electromagnetic field can be used as a medium of measurement through the technique of interferometry which includes a reference fiber that is compared to the sensing fiber to measure the phase difference. The perturbation from the physical quantity can be realized when there is a phase shift between the sensing and the reference fiber [4]. The change in phase is a measure of the change in sensing parameter. Usually, modulation based on phase is more accurate than modulation from intensity [4].

There are two ways in which fiber sensing can work. One is the extrinsic sensing where the fiber acts as the path between the source and the sensor. The modulation due to change in parameter occurs externally by a transducer [4]. Another is the intrinsic sensing where the fiber itself acts as a sensor. The modulation that occurs due to perturbation

of parameter happens in the fiber itself. A brief discussion on these sensor types are as follows

Intrinsic sensor: Fiber acts like a sensor in this kind of sensing technique and it is easier to employ them for remote sensing. In addition, it can also be used for distributed sensing up to a distance of 1m [4]. Usually, multimode fibers are employed for modulation of intensity, whereas other parameters are preferably modulated using single-mode fiber. It is important to vary the optical fiber characteristics to modulate the optical signal propagating through it. Various arrangements of optical fiber for intrinsic sensors are optical fiber grating and the hollow core fiber which are sensitive to perturbations. The modulation in intensity is widely used due to its simple configuration. The output signal attained from the end of the fiber is utilized for interpreting the perturbations from environment.

Extrinsic sensor: An external sensor head is used for sensing physical parameters. Optical fiber is used to transfer information through the sensing region. Optical signal from the sensing region is measured in terms of intensity or phase modulation. This type of sensing helps to measure physical quantities that is difficult to be accessible for sensing purposes using other conventional sensors. Noise protection can also be achieved in this sensing technique which helps to attain accurate results.

Design of a fiber optic sensor depends on numerous factors. It is important to achieve high sensitivity and accuracy from the sensing target to acquire better performance. Apart from the optical fiber, the source and the detector also play an important role in improving the results. Source and detector are always chosen based on the application for which sensing is performed. There are various physical measurands like temperature, vibration, strain, humidity, liquid level and chemical sensing that optical fibers can measure. Usually, intensity modulation techniques are the simplest configuration in which the spectral transmission or absorption changes are noticed as a result of change in the measurands. The phase-modulated technique as mentioned above is also used for measuring extrinsic sensors using interferometric based principle.

Fiber optic sensing based on RI modulation was established in 1970s through simple measurements techniques such as fiber Bragg grating [19] where the periodic distance between the grating and effective refractive index depends on the spectrum that is reflected back as seen in ***Figure 2.4.*** for strain sensing. Other approaches of sensing were investigated using the interferometric technique. One such example is the investigation of Sagnac interferometer for the design of accelerometer for railway purposes using PCF fiber as seen in [20]. Also, sensing with Mach Zehnder interferometer using PCF fiber involved for RI measurement was a widely used approach for sensing. Recently, there

has been new approaches for sensing RI changes. It is sensing based on evanescent wave effect which can be viewed as the interaction between electromagnetic field propagating through the fiber with the surrounding medium. The RI difference between external region and the fiber can cause absorption or scattering of light.

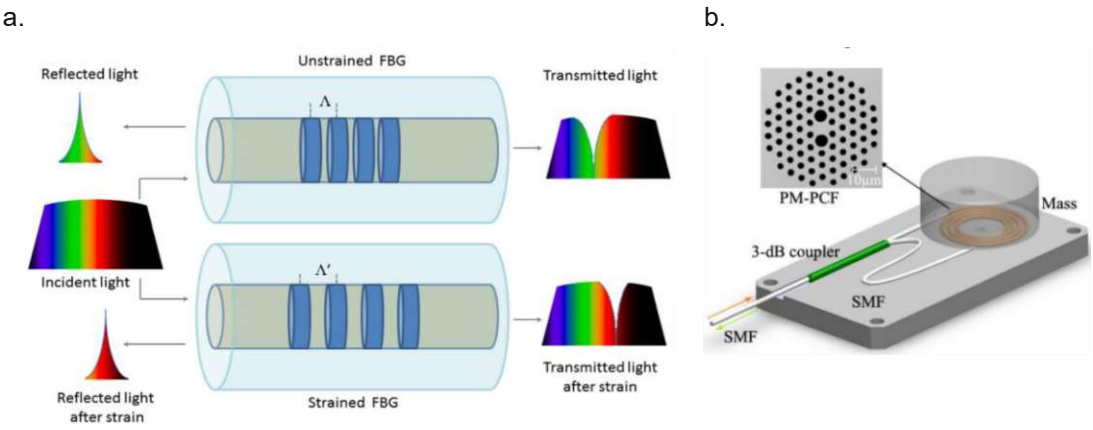

Figure 2.4. *Sensing with a). Fiber Bragg grating (adapted from [19]) and b). Sagnac interferometer (adapted from [20]).*

These recent work shows improvised techniques to measure and sense physical parameters. Different sensing approaches have been carried out like the evanescent wave sensing [21], surface plasmon resonance (SPR) [22]. Optical sensing based on SPR described by Shevchenko et al. [22] uses gold coated optical fiber that can excite surface plasmon resonance using titled fiber Bragg grating (TFBG). TFBG acts like the resonant element which leads to scattering of light from the core to the surface of fiber. The change in SPR is correlated with the change in physical quantity to be measured. For the course of the thesis, we would be focusing on evanescent wave effect-based sensing. A measurement system for optical sensing consists of signal condition component, a sensing element and a signal processing component.

2.5 Sensors based on evanescent wave effect

Evanescent wave effect-based sensing focusses on interaction of electromagnetic energy with the surrounding medium due to leakage of light energy at the core cladding interface during total internal reflection [11]. Evanescent wave effect can be understood using the ray theory approach with phenomena of TIR. As seen in ***Figure 2.5.*** the penetration of evanescent wave at the core cladding interface occurs at each point of TIR in the fiber and a small amount of energy is radiated at the interface. The phase shifts and

the electromagnetic field that decays can be understood with the wave theory. The wave equation given in *equation* (**2.6**) [23] shows that the energy from the evanescent wave is exponentially decreasing as it propagates away from the fiber.

$$E_z = E_0 e^{-\frac{z}{d_p}} \tag{2.6}$$

where z is radial distance from the core, E_z is the field amplitude at distance z, E_0 is the maximum field amplitude and d_p is the penetration depth of evanescent field.

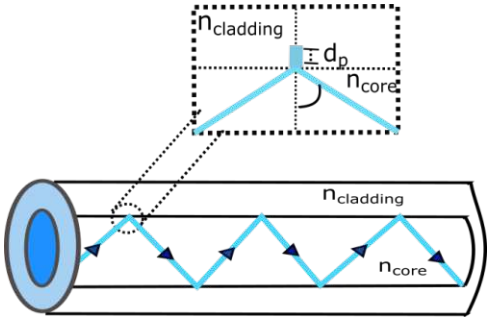

Figure 2.5. *Evanescent wave absorption where the light energy propagates at the core cladding interface (adapted from [11])*

The decaying electromagnetic field at the interface penetrates into the surrounding medium and hence it is also important to understand the boundary conditions of these waves from the fiber. RI of core and cladding plays a significant role in the design and operation of these sensors. Mostly for theoretical analysis of evanescent wave sensor, only meridional rays are considered and often skew rays are neglected for simplification. This leads to simpler calculations and also in the thesis, we also do not take into account the skews rays. The principal factors that need to be considered for design of optical sensors are the type of source of light used, fiber geometry (e.g., straight fiber, U-bend fiber, tapered fiber), the length of fiber used for sensing, the RI contrast and also the angle at which light is launched [23]. The next section focusses on the parameters that are important to enhance the evanescent wave for sensing application.

2.5.1 Evanescent wave parameters

Parameters that mainly affect evanescent based sensing are the penetration depth and the fractional power [11].These sensing parameters can be improved through investigation of physical, optical and geometrical aspect of fibers. The modifications in the fiber are implemented to enhance the evanescence in order to improve the sensitivity of the sensor.

Penetration depth: The penetration depth of the evanescent wave can be defined as the distance at which the amplitude of electric field reduces to 1/e its value at the interface [11]. The penetration depth is given by *equation* (**2.7***).*

$$d_p = \frac{\lambda}{2\pi n_1^2\sqrt{sin^2\theta_i - sin^2\theta_c}} = \frac{\lambda}{2\pi\sqrt{n_1^2 sin^2\theta_i - n_2^2}} \tag{2.7}$$

where d_p is known as the penetration depth, λ is the wavelength of light, n_1 and n_2 are the RI of core and cladding respectively, θ_i is the incident angle and θ_c is the critical angle. It is clear from *equation(2.7)* that penetration depth increases as the contrast of refractive indices at the core-cladding interface decreases [11]. Evanescent wave can interact with the molecules from the surrounding medium at a distance that is detectable by the molecules, this distance which is generally very small is termed as the penetration depth. This leads to reduction in the output power from the fiber end and the light energy leaked in the form of evanescent field can be utilized for efficient sensing. The output power of a multimode fiber can be given by *equation (***2.8***)* [23] which shows the relation with the length of uncoated portion to the output power.

$$P_{trans} = P_o exp\,(-\gamma_{eff} L/D) \tag{2.8}$$

where P_o is the reference power with no changes in the fiber, D being the core diameter of the fiber, L is the active length which is uncoated and is used for sensing. P_{trans} is the power obtained at the fiber end, γ_{eff} is the evanescent wave absorption coefficient. The number of reflections per unit length undergone by a guided ray propagating through the fiber and also the Fresnel's transmission coefficient at the core uncoated interface determines the value of γ_{eff} [24]. The change in output power can be used in sensing applications as a method of measurement, for example, it can be used in fiber optic evanescent wave spectroscopy [25] where the output intensity varies depending upon the analyte which measures the change in RI. RI being a function of parameters like temperature, humidity acts as an optical property useful for sensing application. Thus, penetration depth of evanescent wave affects weaker cladding modes that radiate out, uncoating the fiber helps to capture these waves more efficiently leading to improvement of fiber sensitivity.

Evanescent power: The fractional power in the cladding plays an important role to understand the evanescent field power. This can be given as shown in *equation (***2.9***)*

$$\frac{P_{cladding}}{P} = \frac{4}{3\sqrt{M}} = \frac{4\sqrt{2}}{3V} \tag{2.9}$$

where $P_{cladding}$ is the optical power in the cladding and P being the optical power in the fiber including the core and cladding, M is the number of modes in the fiber and V is the normalized frequency.
From the equation above, it is clear that increase in the normalized frequency will lead to decrease in fractional power in the cladding.

V number mismatch: Another loss that fibers can encounter while used for sensing application is the V number mismatch. When fiber with higher NA_1 propagates to a fiber with smaller NA_2, in this case the higher-order modes from the first fiber are not supported by the receiving fiber which leads to loss of higher-order modes. The power lost (P_L) can be given as shown in the *equation (2.10)*

$$P_L = -10log\,(\frac{NA_2}{NA_1})^2 \tag{2.10}$$

V number mismatch occurs in the fiber when used for sensing applications. The fiber is uncoated which leads to mismatch in V number between uncoated and the other region of fiber. Thus, there are losses of higher-order modes when light travels from uncoated fiber to coated fiber as shown in ***Figure 2.6.***

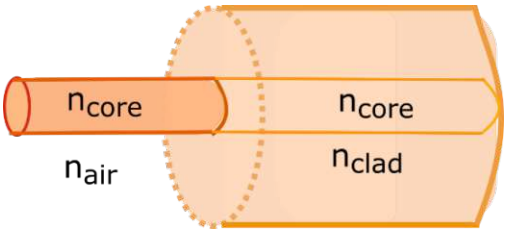

Figure 2.6. *V number mismatch due to dissimilarity in cladding material leading to difference in the modes propagating through the fiber.*

2.5.2 Factors affecting sensitivity of fiber optic sensor

Penetration depth and fractional power are two important factors that affect sensing performance. There are different optical parameters which control these factors. The variations in these optical parameters are investigated to improve the sensing performance. The parameters include the adjustment of incident angle, incident wavelength of light source and sometimes also the fiber characteristics like the geometry of fiber.
Incident angle: Penetration depth of evanescent field can be increased by increasing incident angle. The penetration depth is highest when the incident angle is near the critical angle. This can be achieved by changing the launching angle such that incident angle is closer to critical angle.

Wavelength of light source: The next parameter that affects evanescence is the input wavelength of light source. Penetration depth can be increased with longer wavelength. Thus, it is preferred to use IR laser sources for evanescent wave effect-based sensors.

2.5.3 Geometry of evanescent wave sensing

Straight geometry fiber sensing: The next factor that can affect the penetration depth is the geometry of optical fibers. Geometry of fiber sensing can vary from straight fiber to U-bend fiber and tapered fiber. Straight fibers are the simplest design for sensing application with robust performance. The sensing capability can be improved by increasing the length of uncoated region such that more evanescent wave interaction can occur with the surrounding medium as in this case there are more TIR points during propagation of light. A simple model was proposed by Wu et al. [26] where theoretical analysis was performed to study the effect of core diameter, the conditions for launching the light and the RI of the surrounding medium. These factors help to calculate the penetration depth of the evanescent wave. Fractional power was also investigated theoretically in order to understand the limit for sensing a particular analyte. Sensing of water level was investigated by Golnabi et al. [27] where the main focus was to check the stability of the designed sensor and to improve the efficiency of the device. Analytes which serve as surrounding medium to fibers have an effective RI, the change in effective RI leads to modulation of intensity which can be measured to understand the sensing effect. In these fiber designs, the fiber is uncoated and the nature of light transmission is studied. Light propagating through fiber around air has a different condition for TIR compared to light propagating through fiber which is surrounded by a liquid of different RI than air. In this case, the energy loss is measured to understand sensor's response. The losses encountered during propagation and coupling needs to be considered for analysis of sensing. Various sensors are designed using straight geometry for liquid sensing. Another example was developed by Xiong et al. [28] to measure concentration of nitrite in sample water. Nitrite concentration was considered as a measure of evanescent wave absorption. It was a linear relation with a limit of detection as 0.02 mgL^{-1} [28].

It is also important to choose a cladding material for fabrication of fiber as it effects the evanescent wave propagation through the cladding. There are certain requirements which needs to be satisfied while selection of cladding material for fiber sensing. The cladding material at wavelength of propagation should be transparent such that there is no damage. Adequate thickness is also an important factor as it helps to allow evanescent wave to decay to a level such that it is not exposed out of the cladding. This helps to preserve the light through the fiber in the remaining part where there is no sensing.

Thus, core and cladding are fabricated from glass to give a better performance than cladding made from other materials.

U-bend geometry: The next type of fiber geometry is U-bend geometry where the sensing part is bent in form of U shape so that the penetration depth increases and improves sensing performance. This geometry gives better performance as it increases the evanescent wave effect in the bend region. The bending causes the modes to shift outward of fiber leading to higher evanescence and better sensitivity as seen in ***Figure 2.7b.*** There is also possibility that some modes are lost when the fiber is bend, this depends on the bend radius and fiber width. When modes are lost, it does not help in sensing performance whereas it is the modes shifting outwards which helps to improve the penetration depth as seen in ***Figure 2.7a.*** The ray theory explains the improvement of sensitivity as the total internal reflection points increase in the bend region guiding light to cladding and thus increasing the evanescent field in comparison to straight fiber geometry. U-bend sensor is widely used due to its higher sensitivity. Some of the recent applications with U-bend fiber are sensing parameters like strain [29], humidity where higher range of humidity was sensed efficiently with U-bend structure [30]. Gas sensing with SnO_2 coating provided an accurate sensor response for H_2 gas detection in high temperature conditions [31]. It also was used for sensing heavy metal ions [32] and even Covid-19 [33].

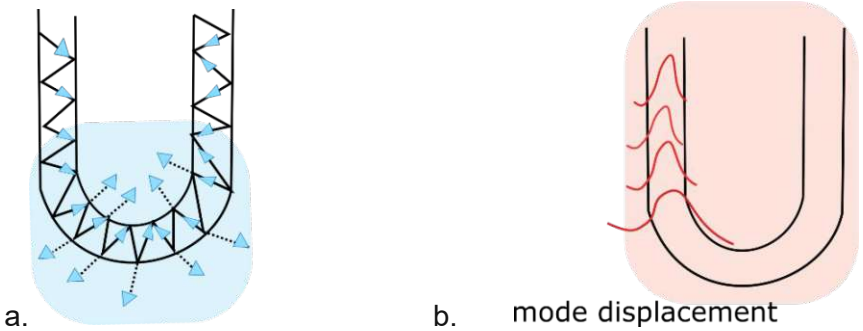

Figure 2.7. *a). U-bend fiber exhibits higher losses and thus has evanescent field intensity. U-bend increases the TIR points in the fiber. b). The modes shift outward when the fiber is placed in U bend shape which increases the evanescent field in the U-bend region.*

U-bend sensing unlike straight fiber sensing also involves the need to analyze the electromagnetic field propagating through the inner bend radius or the outer bend radius. With decrease in bend radius, there is increase in penetration depth as seen in few examples [34]. Below the optimum radius, there is possibility of cross coupling [35] which leads to lower the sensitivity of evanescence absorption [36]. Optimum radius can be achieved by controlling NA and core diameter of fiber. The importance of core diameter

for sensing performance was demonstrated by Ruddy et al. [37] where evanescence was better for a multimode fiber having diameter 200 µm with length of 20.5 cm for uncladded fiber compared to fiber diameter 600 µm with length 22 cm for measurement of methyl blue concentration. Another parameter that needs to be analyzed is the NA since it is different in U-bend part of fiber. Also, coating of fiber can alter the sensing performance. The change in the light propagation that occurs with coating the fiber has influence on the evanescent wave effect. Thus, there should be an optimum estimation for these parameters to obtain a maximum possible sensing performance. In the study of U-bend structure, it is equally important to include the analysis from skew rays which are mostly neglected. There are examples [38], [39] where skew rays are included as it covers large range of incident angle and helps in improving evanescent wave effect. This leads to efficient investigation of sensing performance.

Tapered geometry: Tapering of fiber increases evanescent wave effect and helps to attain greater sensitivity compared to straight fiber geometry. Tapering of fiber leads to increase in electromagnetic energy in the cladding region. Adiabatic tapering is the process carried out to avoid coupling of higher-order modes by keeping the taper angle small. The phenomena of TIR increases with tapering and increasing evanescent power. This type of sensing is advantageous in itself as it reduces the *V* number mismatch and helps to build the sensor performance. The penetration depth of evanescent field with tapered geometry is high as seen in ***Figure 2.8***.due to reduction in the fiber diameter in the sensing region. Light guided in this region with reduced waist diameter encounters larger interaction with the analyte.

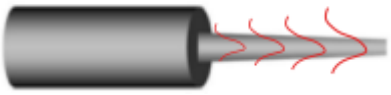

Figure 2.8. *Tapered geometry to improve sensing performance in fiber optic sensor.*

Tapering is basically performed by pulling the fiber during heating in such a way that the resulting diameter is less than the actual core diameter of fiber. It also depends on the length to which tapering is performed and the effect of coating which can influence the sensing performance. It is generally difficult to fabricate and the process makes it fragile when the tapered fiber is formed from uncoated fiber. Some examples are when tapering is performed with fibers that is coated with nanolayers of poly R-478 and poly diallyldimethyl which can sense humidity for the range from 75% to 100% [40]. These coated layers help to trap water which can help in sensing humidity. The length and tapered diameter

were optimized to obtain highest sensitivity. Another example of tapered geometry is sensing of methylene blue for different concentration such that the absorbance is increased with decrease in tapered diameter [41]. The RI of analyte was regulated to obtain high interaction of light with surrounding medium.

Different materials used for fabricating fibers also affect to an extent the sensing performance. Mainly used materials are glass or plastic fibers. It is noticed in various applications that usage of plastic fiber leads to high robustness and mechanical stability, more flexible in use, has lower bend radius while used in U-bend geometry [38]. Also, with high NA of plastic fibers, it is easier to couple light into it as this enhances sensor sensitivity. But plastics fibers have lower glass transition and melting temperatures that can range between 80°C to 100°C. If these fibers are subjected to constant high temperature, it can make fibers turn brittle and not useable for sensing purposes. There are optical transmission losses as these fibers also absorbs moisture from the surrounding [35]. On the other hand, glass fibers are brittle and have lower mechanical strength which affects its performance. But it has higher melting temperatures and are not subjected to any kind of external disturbances. Since humidity and temperature influence sensor performance, it is important to study the effect of these parameters on fiber to understand the materials suitable for various application.

2.6 Femtosecond lasers

Femtosecond lasers were developed in early 1964 where the need to have short pulse duration for different applications became the driving force to generate it [42]. The first-generation pulsed lasers were generated with mode-locked technique from lamp solid state lasers, dye lasers or gas lasers to form pulses less than 100 picoseconds. Later, the discovery of continuous-wave (CW) organic dye laser [43] led to the beginning of second-generation mode-locked lasers produced as a tunable broadband laser. Also, the use of slow saturable absorber in passive mode-locking created an advancement in the development. With intense research on the pulses formation and pulse shaping mechanism from mode locking led to development of ultrashort pulses up to 100 femtoseconds. Later semiconductor lasers were utilized for the same purpose and these were the basis for the revolution to the third-generation femtosecond lasers. Ther major breakthrough for the third-generation mode locked laser was the utilization of optical Kerr effect where Kerr lens was used as a saturable absorber, which is a transparent medium generating instantaneous short pulses. The other breakthrough was the development of la-

ser media like Ti:sapphire which is a tunable laser [44]. There were further more developments in order to reduce the complexity and improve the performance of ultrafast laser. The exploitation of ultrafast lasers makes it widely acceptable due to its reliability, high reproducibility in its performance. The design and development of ultrafast lasers leads to its effective usage in various applications. They are used to probe ultrafast processes that occurs in nature like chemical reactions where one can excite chemical bonds and control the molecular vibrations and lead to formation of desired compounds. It can be used in the medical field for vision correction [18], for optogenetics where the neurological signals can be controlled using light signal for different activation or inhibition of genes [45].

Ultrashort laser pulses are of interest due to generation of laser pulses with durations ranging from picosecond (10^{-12}) to femtoseconds (10^{-15}). Pulsed lasers can either be short or long pulse depending on the time duration of pulse generated as seen in ***Figure 2.9***. Short pulses have broader spectrum and long pulse have narrow spectrum which is explained with the Fourier transform. The uncertainty principle says that the product of temporal and spectral width is great than ~1. Pulsed lasers are generated using the technique of mode-locking.

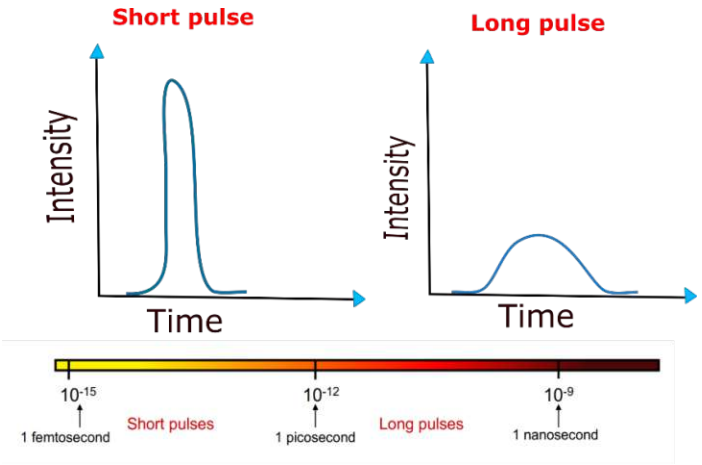

Figure 2.9. *Short pulse ranges from time scale of picosecond to femtosecond and long pulse range from nanosecond to few picosecond*

Femtosecond lasers are generated through mode-locking technique. Lasers have a finite spectral bandwidth, let's say Δv but it is present in discrete frequencies or so-called modes v_m in laser cavity. Each mode in the cavity is separated by mode spacing δv which is given in *equation (**2.11**)*.

$$\delta v = \frac{1}{T} = \frac{c}{2L} \qquad (2.11)$$

where *T* is the cavity round trip time, *c* is the speed of light and *L* is optical cavity length. In general, the laser spectrum has its frequencies oscillating in random phase resulting in an incoherent output in the form of random fluctuations having no temporally defined structure. At certain timescale when the modes of laser oscillate in phase, there is a sudden increase in intensity due to constructive interference between the modes leading to the formation of a coherent spike. Thus, locking of modes together can help to create pulsed lasing with short time duration as seen in ***Figure 2.10.*** Ultrashort pulses can be created by increasing the number of modes in the cavity. From *equation (**2.12**).* It is clear that increasing the number of modes can reduce the pulse duration of the output pulse.

$$tp = \frac{1}{n\delta v} \tag{2.12}$$

where *tp* is the pulse duration of output pulse*, n* is the number of modes. The number of modes can be given by *equation (**2.12**).*

$$n = \frac{\Delta v}{\delta v} \tag{2.13}$$

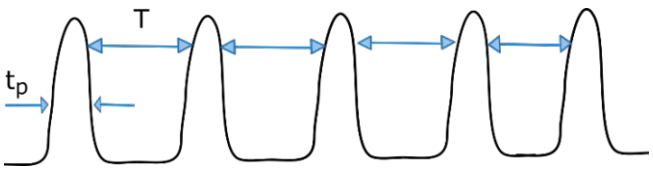

Figure 2.10. *Schematic of mode locked laser pulse*

The output pulse generated from mode-locking ideally is described as transform limited pulse. The time bandwidth product of mode locked output pulse is the product of time duration of pulse (tp) and the spectral bandwidth (∆v) at full width half maximum (FWHM) which is equivalent to a constant k that depends on the shape of pulse. For a gaussian shape, k is 0.441 and for secant square pulse it is 0.316 [44]. It helps in identifying a transform limited pulse from other forms of pulses as the constant k value increase when the pulse is not transform limited.

There are two types of mode locking known as the active mode-locking and passive mode-locking. Active mode-locking uses an external signal to modulate the signal from laser source to get the modes locked. Whereas in passive mode-locking, the laser source itself generates a modulation through a nonlinear material forming mode locked pulses which matches with the cavity round trip frequency.

Active mode-locking: Active mode-locking can be achieved through modulation in different ways such as the amplitude mode-locking and the phase mode-locking. This can be done with coupling the modes externally and stimulating oscillation that are in phase. Coupling of modes can be done for example using an acoustic optic modulator which causes time-varying amplitude change or an electro optic modulator which produces time-varying phase modulation. The active modulator with a modulation frequency Ω generates sides bands on the laser modes such that it is equal to the laser cavity mode spacing. The mode-locking condition can be achieved using *equation (**2.14***). Thus, the modes are now coupled together and can oscillate in same phase as seen in ***Figure 2.11***.

$$\Omega = \frac{c}{2L} \tag{2.14}$$

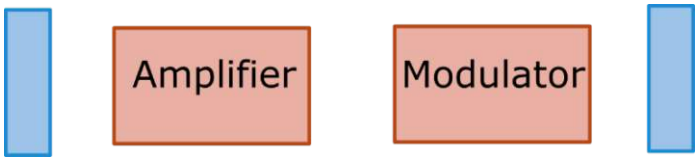

Figure 2.11. *Active mode-locking*

Passive mode locking: This type of mode-locking can be achieved when the laser can itself modulate the signal to cause locking of modes as seen in ***Figure 2.12.*** It is also referred to as self mode-locking due to the amplitude modulation that is incurred by the laser itself without any external element. This is mostly carried out by saturable absorbers. Saturable absorbers for example are made of cyanide dyes. The saturable absorber material absorbs the photons from laser into the material until a stage reaches that it can no longer absorb. At this stage, the population at the ground state of the material will be equal to the population of excited state. Thus, this condition makes the material to behave like a bleached system or a transparent system in which the light will pass through the saturable absorber without any absorption. Finally, we can say that the saturable absorber behaves opaque when the intensity of light passing through it is low and behaves like a transparent material in case when intensity is high. But phase correlation is achieved when the gain is more than the losses and this occurs when the saturable absorber is bleached and allows light to pass through without losses. Also, it is important to note that the pulses generated from passive mode locking is shorter than active mode locking.

Figure 2.12 *Passive mode-locking*

Another category of femtosecond lasers that has widely grown over the years is the fiber laser technology. Ultrafast processes have been utilized in optical fiber way long back before the start of laser fiber technology. 20 years before the beginning of fiber laser, ultrafast lasers which were huge in size were exploited in optical fibers making the whole system bulky and not portable. In recent years, with the discovery of fiber lasers, it is now possible to have it as a compact system which is used for wide range of applications. Additionally, fiber lasers eliminate the thermal lensing problems which leads to added advantages. Beam quality can be improved based on fiber core design and does not involve the dependence of other parameters. The first type of fiber lasers were the single-mode rare-earth doped fibers [46] and diode pumped single mode fiber lasers [47]. With the usage of semiconductor lasers, there is increase in average power levels that can be achieved from fiber laser [48]. Thus, the discovery of fiber laser technology has led to exploitation of a robust large-bandwidth and optically integrated solid state laser device.

3. METHODOLOGY

This chapter describes the methodology of sensing physical parameters via a specialty optical fiber. It also presents the design and the optical properties of the applied extrinsic sensor system. Extrinsic fiber optic sensor has gained significant importance in the last few years due to its ability of distributed sensing and high sensitivity. Generally extrinsic sensing is performed with standard fibers used for telecommunication, however we used a D-shaped fiber which was specially designed for sensing applications.

3.1 Laser source

The guidance of electromagnetic field in coherent sources through optical fibers is standardly ensured at high transmission levels and beam quality. Lasers are typical representants of such sources which provide stable output allowing to establish the necessary signal sensitivity. Laser with infrared operation wavelength was chosen for this work because the evanescence wave effect improves with wavelength.

We used a femtosecond Ytterbium-based fiber laser source at near infrared wavelength (NIR) with 1030 nm center wavelength, 100 MHz repetition rate and 100 fs pulse duration. The average power of such source is 10 mW at 0.24 A current level of the pumping laser diode. The main objective to use a femtosecond laser was to study the sensing potential in a broader spectral range. ***Figure 3.1.*** shows the spectrum of laser source at different laser diode current. The narrow band extraordinary peak of the spectral curve in ***Figure 3.1.*** at 0.19 A indicates unstable operation with partial continuous wave (CW) effect. However, this transient imperfectness disappeared at slightly higher pumping powers enabling stable operation at 0.24 A.

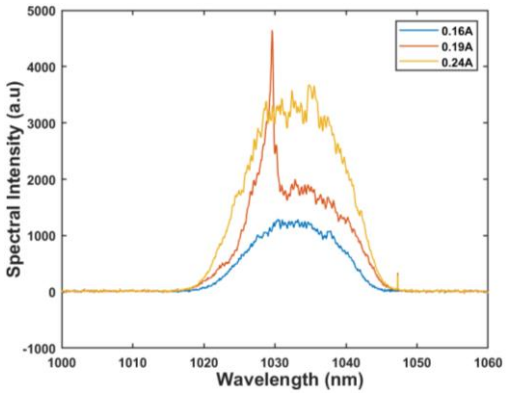

Figure 3.1. *Spectrum of the ultrafast laser source depending on the pumping laser diode current.*

Some laser beam parameters were measured in order to ensure its efficient coupling into the fiber for proper sensing performance. An important parameter is the laser beam size, which besides the wavelength determines the optimal focal length of the in-coupling optics. The beam size of laser was found out by beam profiler camera allowing real time monitoring of the diameter giving value 1 mm at $1/e^2$ level with negligible ellipticity as seen in ***Figure 3.2.***

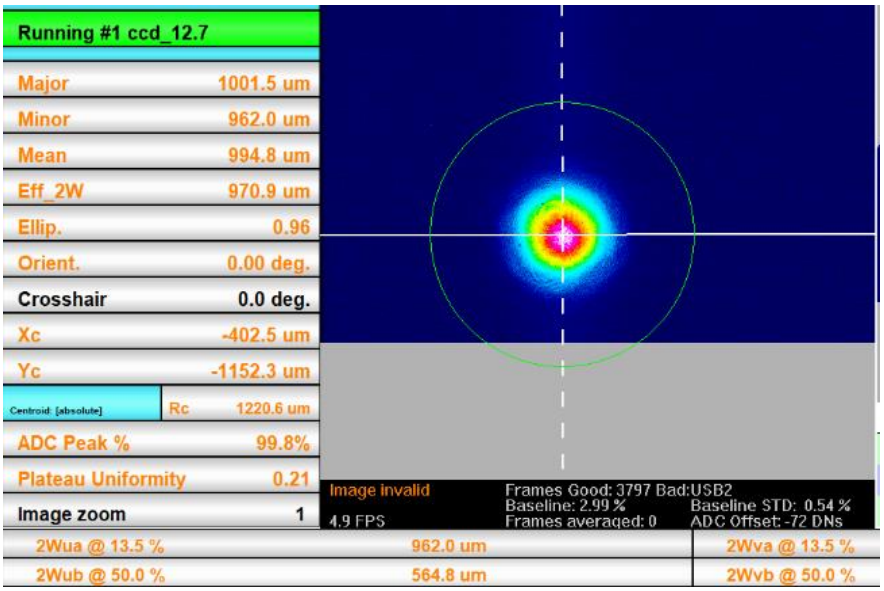

Figure 3.2. *Beam profiler measurement output of the laser beam together with the identified beam geometry parameters.*

Another essential parameter to be considered for sensing purpose is the polarization status and it has LP character with electric field vector orientation of 54 deg in relation to the laboratory vertical axis. Thus, the output has a mixed polarization having a vertical and horizontal component. $\lambda/2$ waveplate was used to rotate the existing polarization orientation of the field to horizontal or to vertical polarization direction, because the anisotropic fiber input facet was oriented also in relation to the main laboratory axis.

3.2 D-shaped optical fiber

A specialty D-shaped optical fiber was used in the sensing application experiments developed and manufactured by group of prof. Buczynski in Lukasiewicz Research Center-Institute of Microelectronics and Photonics in Warsaw. It is important to stress that the fiber cross section in form of letter D was achieved not via post processing of a standard spherical shape. A new technology approach was applied by which the fiber expresses homogeneous D-shape cross section along the whole length after the drawing process. In ***Figure 3.3.*** scanning electron microscope (SEM) image of the fiber cross section is

presented expressing 106 µm diameter of the spherical shape part and 54 µm thickness of the cladding along the symmetry axis crossing the fiber core. The core exhibits slight ellipticity with dimension 8 µm and 7 µm along the symmetry axis and in direction perpendicularly on them, respectively. The evanescent wave effect is ensured by the thin cladding towards the flattened surface of the cladding with dimension about 2 µm.

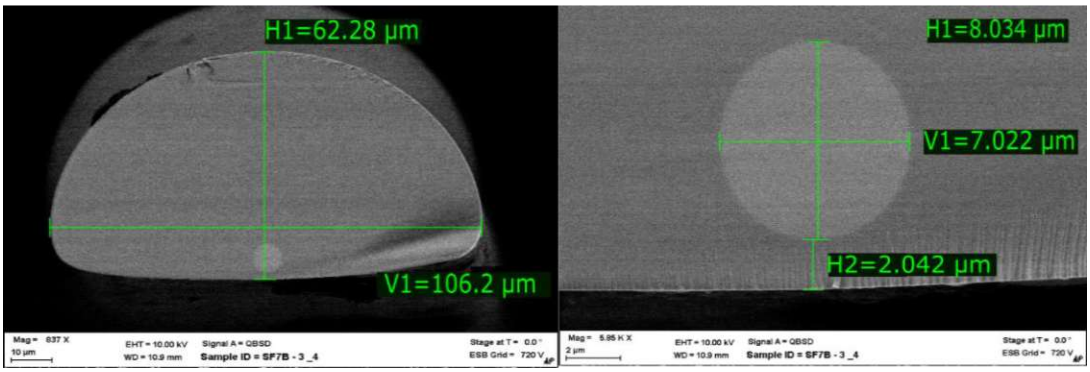

Figure 3.3. *Scanning electron microscope images of the D-shaped fiber cross section together with dimensions of main geometrical parameters.*

The parameters of the fiber play an important role in determining the optical sensing effect. The cladding is made of a silica glass and has a RI of 1.45 at 1030 nm. The core is made of germanium doped silica glass with a RI of about 1.453 at 1030 nm. During sensing experiments, fiber samples with length 20 cm and 50 cm were used in straight configuration and the longer samples were arranged for U-bend geometry. The fiber was uncoated in the center region along length of 4 cm in order to ensure direct contact with the surrounding liquid medium which was the analyte under study. The uncoated process was performed by placing the central region of the fiber into acetone for 1 hour to soak the acrylate coating material before its mechanical removal. The fiber ends were also soaked and uncoated in order to clean and cleave them. The careful cleaving process was necessary to ensure effective in-coupling of the laser radiation and its out-coupling towards the detection technique. In-coupling was managed for the experiment with the free beam and lens configuration. Whereas, the outcoupling was from lens or through direct contact with butt coupling technique. Direct contact was incorporated for spectral measurements using a multimode collection fiber with core size of 200 µm or 400 µm connected to the spectrometer.

The focal length of lens used for effective in-coupling of the free laser is calculated using *equation (*2.5*)* at assumption that the beam diameter at the fiber input should be 66% of the core diameter. Taking λ=1030 nm, beam quality factor M^2=1 and average core diameter 7.5 µm, the optimal focal length with f= 4 mm was used for in-coupling.

The output lens was used for monitoring of the spatial field distribution at the output fiber facet using Wincam silica-based beam profiler. The image distance and object distance were adjusted in order to ensure sufficient magnification of the image in relation of the camera chip pixel resolution. After proper alignment of the in-coupling and out-coupling geometry a slightly elliptically shaped field distribution image with symmetric and single peak character was observed as presented in ***Figure 3.4.***

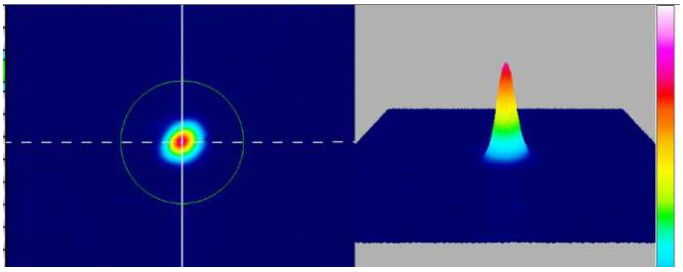

Figure 3.4. *Electric field intensity spatial distribution at the output facet of a D-shaped fiber.*

Due to the fiber core ellipticity and thin cladding situated only towards one direction from the core it expresses anisotropic character, which ensures polarization maintaining functionality. The core of this fiber is at 2 μm distance to the flat edge of D-shaped cladding. We oriented the fiber ends both at the input and output to ensure that the cross-section symmetry axis of D-shaped fiber coincides with the laboratory vertical direction. It means, that in case of vertical and horizontal laboratory polarization settings, this polarization orientation was preserved during the whole propagation length regardless of the twisting deviations. The electric field vectors for both horizontal and vertical polarizations is shown in ***Figure 3.5.*** The diagram above is schematic representation of the results obtained via the camera (below). Such polarization maintaining character allowed to analyze the polarization effect during the sensing experiments as well.

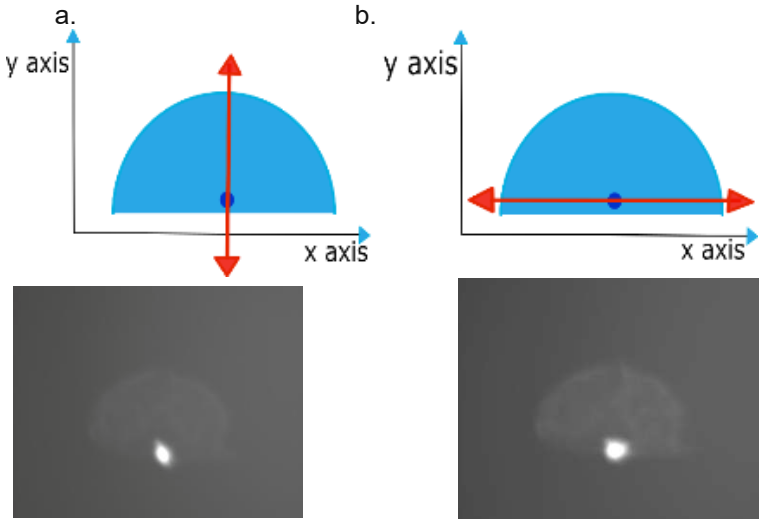

Figure 3.5. *Polarization through D-shaped fiber with electric field vector direction as a). vertical polarization b). horizontal polarization.*

The sensing experiment was carried out in two main geometrical arrangements of the optical fiber

- Straight fiber geometry is the simplest arrangement that can be exploited for sensing experiments with potential RI sensitivity. The change of RI around the cladding of fiber to higher values than related to air has potential effect on the transmission characteristics. Sensing can be studied in this case by collecting the transmission signal and can be improved by controlling the fiber length immersed into the liquid analyte.
- Further, U-bend geometry is used for sensing experiments, because the modes propagating in the U-bend region are deformed due to the enhanced evanescent wave effect. But U-bend region forms often a fragile geometrical setup which makes difficulties in the signal stability and reproducibility. Sensing with U-bend geometry can be an improved by decreasing the U-bend radius to ensure enhanced penetration of the field beyond the fiber cladding.

The D-shaped fiber due to its asymmetry does not have uniform width causing a difference in sensing performance. Standardly in straight fiber geometry, the whole sensing region is immersed into the analyte. This does not affect the orientation of the D-shaped fiber used for sensing. Whereas, in case of U-bend, it is important to check the orientation of the fiber such that higher evanescent field is exhibited at particular orientation. ***Figure 3.6.*** shows the fiber's longitudinal section under optical microscope with illumination from the top to understand the asymmetry of D-shaped

fiber. The core was orientated towards through manual rotation of the fiber and constant inspection with microscope to check the amount of rotation until the desired orientation was achieved. The main drawback in this case is that fiber has tendency to revert back to a position with core in the inner surface due to tension created in the fiber.

Figure 3.6. *Longitudinal section of a D-shaped fiber in the U-bend region at different curvature position under optical microscope.*

Both the geometrical arrangements were studied to compare their effect on the spectral sensitivity of different analytes. This fiber acts like a multimode fiber below the cutoff wavelength.

The V parameter for the D-shaped fiber is given by *equation (2.2)*

$$\mathrm{V} = \frac{2\pi}{\lambda}\, a\sqrt{n_1^2 - n_2^2} = 4.27$$

Number of modes, $M \approx \frac{V^2}{2} = 9.36 \approx 9\ modes$

The cutoff wavelength is given by *equation* (2.3*)*

$$\lambda_c = \frac{2\pi}{V_c} a\sqrt{n_1^2 - n_2^2} = 1.840\ \mu\mathrm{m}$$

Thus, the cutoff wavelength is 1840 nm showing that D-shaped fiber behaves like a multimode fiber at 1030 nm.

3.3 Experimental Setup

Analytes studied for the sensing experiment were distilled water and isopropanol. Distilled water is (chemical formula H_2O) free from suspended particles and other impurities through the process of distillation and has high importance in laboratory experiments. It

is odorless, tasteless and is transparent in nature. The RI of distilled water is 1.327 at 1.0 µm. Isopropanol also known as isopropyl alcohol (IPA) has its chemical formula (C_2H_6OH) is a commercially important solvent in many industries. It is mainly used as solvent to extract natural products like gums and oils. The RI of isopropanol is 1.370 at 1.0 µm and is miscible in water. The absorption spectrum of both the liquids were also studied (isopropanol and distilled water) and is shown in ***Figure 3.7.*** Significant absorption was observed in the infrared wavelength region above 1.1 µm. At wavelength 1030 nm only weak absorption was measured with absorbance values 0.024 and 0.0030 for water and IPA, respectively, in the case of 5 mm cuvette.

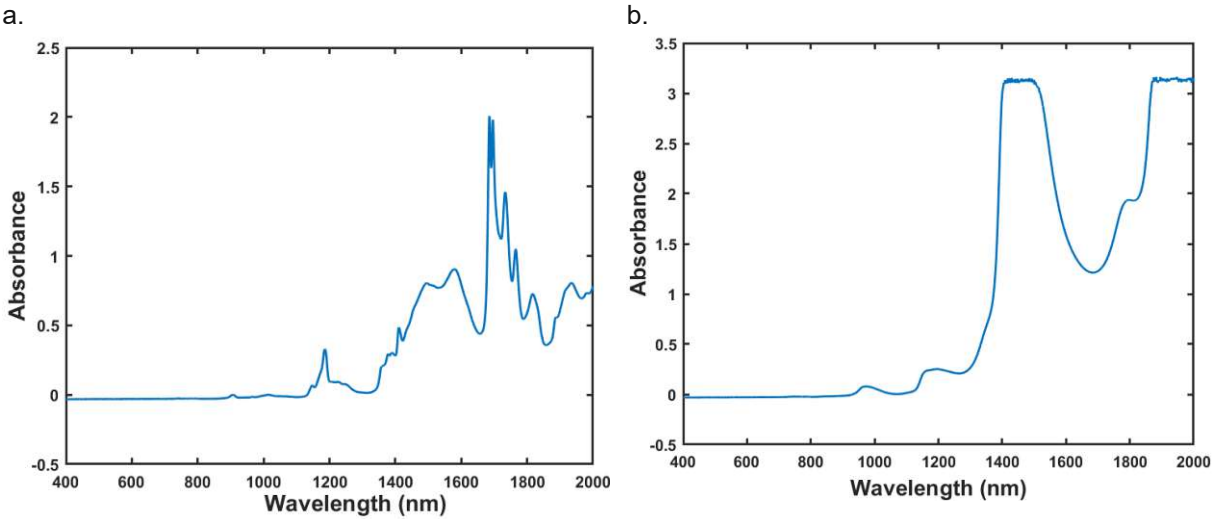

Figure 3.7. *Measured absorption spectrum of the used a). isopropanol and b). distilled water material using 5 mm cuvette.*

Experiments were carried out to study the sensing effect using D-shaped fiber. Chemical sensing was the main goal of experiment which was enabled via interaction of evanescent wave with the surrounding medium. High evanescent field effect under propagation through D-shaped fiber was achieved due to asymmetric cladding structure presented above. During the first experimental series the fiber length 20 cm and its 4 cm part was uncoated in the central area. The sensing measurements were carried out with an experimental setup as shown in ***Figure 3.8.*** The 10-mW average power beam of the fiber laser source is in-coupled into the core of the D-shaped fiber using a lens placed in a 3D micrometric positioning stage. *λ/2* waveplate controls the orientation of beam polarization that enters the fiber. The in-coupling alignment was realized by monitoring of the output fiber facet field distribution using the beam profiler camera. The magnified image of the output facet was enabled by a second short focal length lens placed on a second 3D micrometric positioning stage.

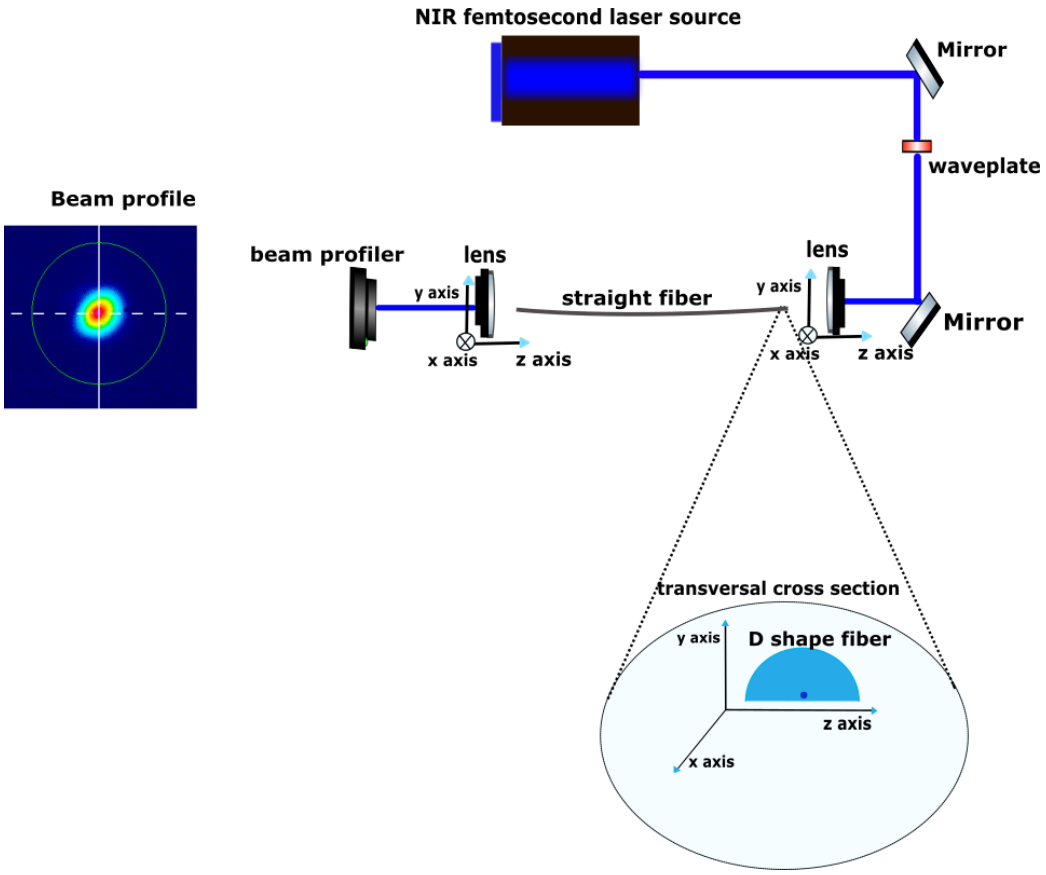

Figure 3.8. *Basic experimental setup used for the optimization of the in-coupling geometry.*

Figure 3.8. shows the input and output orientation of D-shaped fiber facet situated in the transversal plane of the beam propagation. It was rotated around the main fiber axis to have a parallel status of the flat surface of the fiber with the surface of optical bench. The multimode effect of the fibers was analyzed by misaligning the in-coupling geometry from the optimized position in the transversal plane. ***Figure 3.9*** presents the change of the near field image of the fiber output under simultaneous shift of the two transversal alignment screws to left-right and up-down directions. The images express slight change of the output beam profile. The analysis was done for both horizontal and vertical polarization under the same registration conditions. Thus, the lower intensities in the case of vertical polarization unveil higher losses in comparison to the horizontal one. After beam profile analysis, the spectrum of the outcoupled optical radiation was registered by a high resolution spectrometer (Ocean Optics, HR USB 4000, 940nm-1100nm) for both polarizations.

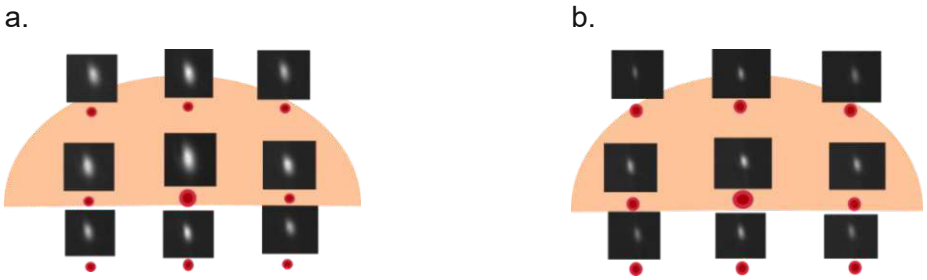

Figure 3.9. *Registration of the input misalignment effect on the output beam profile both for a. horizontal and b. vertical input polarization.*

The above presented registration was performed in dry status of the sensing region, i.e., surrounded by air (RI=1). In the case of liquid spectral sensing, the output lens was exchanged with the spectrometer collection fiber butt-coupled to the D-shaped fibers output end. Then the uncoated region of the fiber was merged to the analytes. Firstly, distilled water was examined, which did not cause any changes in the output spectrum. In contrast, the isopropanol as analyte caused significant homogeneous increase of the spectral intensity in comparison to the original spectrum. The second experimental series was devoted to the increase of analyte in the sensing region of the fiber through step-by-step addition of higher volume of the analyte liquids as seen in ***Figure 3.10.*** It presents the changes of the output spectra under monotonous increase of the length of the uncoated sensing region with step 0 cm,1 cm, 2 cm, 4 cm and the final drying of the uncoated region.

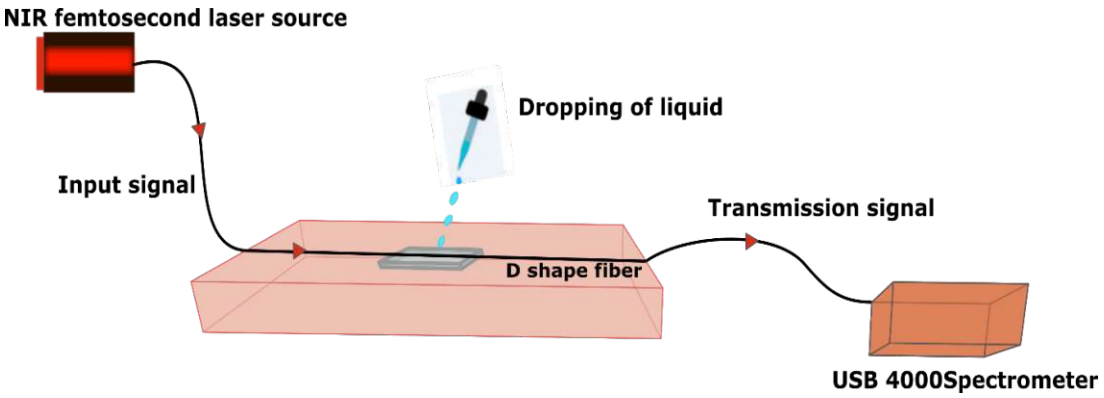

Figure 3.10. *Experimental setup of filling isopropanol in the sensing region through step-by-step addition of higher volume of isopropanol.*

The dropping experiments examined the dependence on the measure of isopropanol surrounded in the sensing region. Isopropanol is considered to be an important chemical in various industry which also makes it important to investigate its purity and any kind of contamination. Distilled water being a non-reactive and miscible liquid can be easily be

a source of contamination in isopropanol. Thus, sensing with evanescent based sensor can be a simple method to identify such impurities. Mixture of isopropanol and water was tested for sensing with D-shaped fiber. The mixture was prepared staring with 1 proportion of isopropanol (volume of 100µm) with 9 proportion of distilled water (volume of 900 µm). Later, the proportion of isopropanol was increased until finally there were 9 proportion of isopropanol (volume of 900µm) with 1 proportion of distilled water (volume of 100 µm). Spectral measurements helped to understand the intensity changes in each case and to identify the measure of contamination with water.

Improvement of sensing performance is an important aspect for efficient working of sensor devices. This can be enhanced by changing the geometrical configuration of the sensing region. U-bend geometry was examined in order to improve the current sensing effect. Another fiber specimen with length 50 cm was taken to study the sensing effect with the same liquids. The length of the uncoated region was preserved to be 4 cm. All above described measurements were performed at laser diode current of 0.24 A and the output collection fiber of spectrometer with core diameter of 200 m was constantly moved in order to smear out the interference spectral peaks. U-bend geometry was inspected to study its effect on sensing performance comparing the obtained results to the straight fiber geometry one. U-bend was prepared manually to have the sensing region bended in the shape of U and held it in the same position while performing experiments for sensing. The experimental setup is shown in ***Figure 3.11.*** where the orientation of transversal position of D-shaped fiber and other parameters are kept the same as mentioned above, only the geometrical structure of the fiber was changed to study the consequence of geometry on sensing performance.

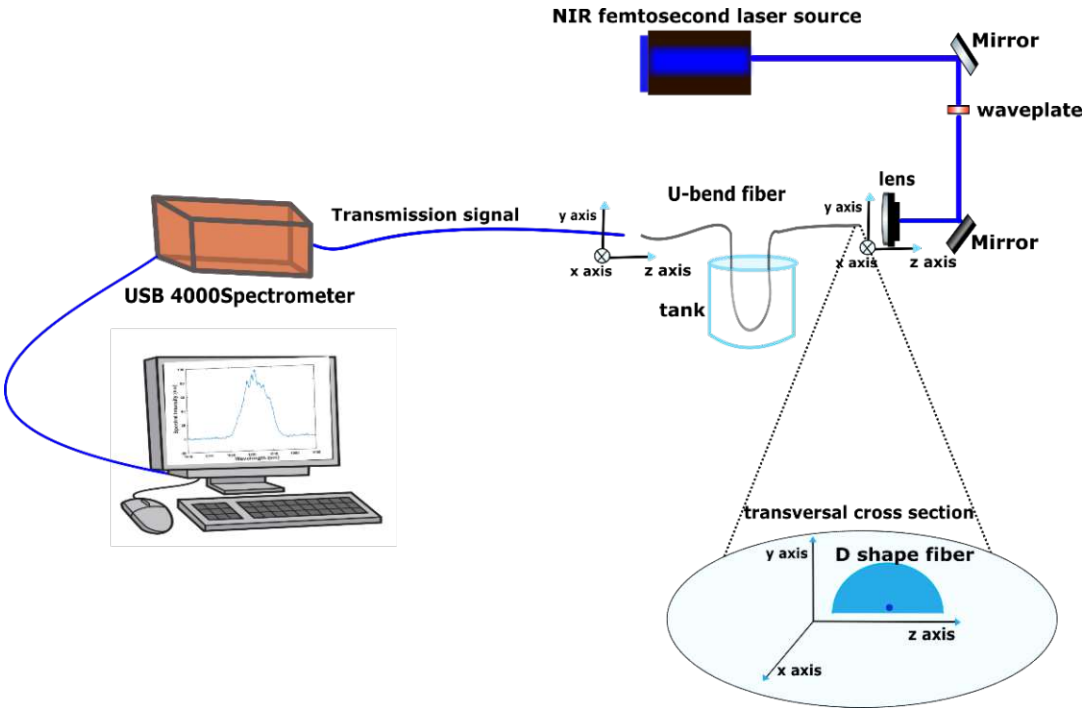

Figure 3.11. *Experimental setup with U-bend geometry of fiber.*

4. RESULT AND DISCUSSION

The sensoric experiment was carried out using several fiber samples from the same fabrication series with cross section geometry presented in ***Figure 3.3.*** The fiber length effect was examined testing 20 cm and 50 cm samples and beside the straight fiber arrangement also the U-bend geometry was exploited in the case of the longer samples. The output signal was registered mainly using spectrometer and, in some cases, also via camera in configurations described above. In the next part of the thesis the obtained results are presented together with appropriate discussions.

4.1 Straight fiber geometry

At first, the outcomes obtained using 20 cm sample in straight geometry with 4 cm uncoated area immersed in the test liquids are listed. Intensity changes in the spectrum were observed through contact of the D-shaped fiber with water or isopropanol medium. The sensing performance expressed polarization dependence, which is presented on spectra registered for both horizontal and vertical input polarization in case of isopropanol medium as seen in ***Figure 4.1.***

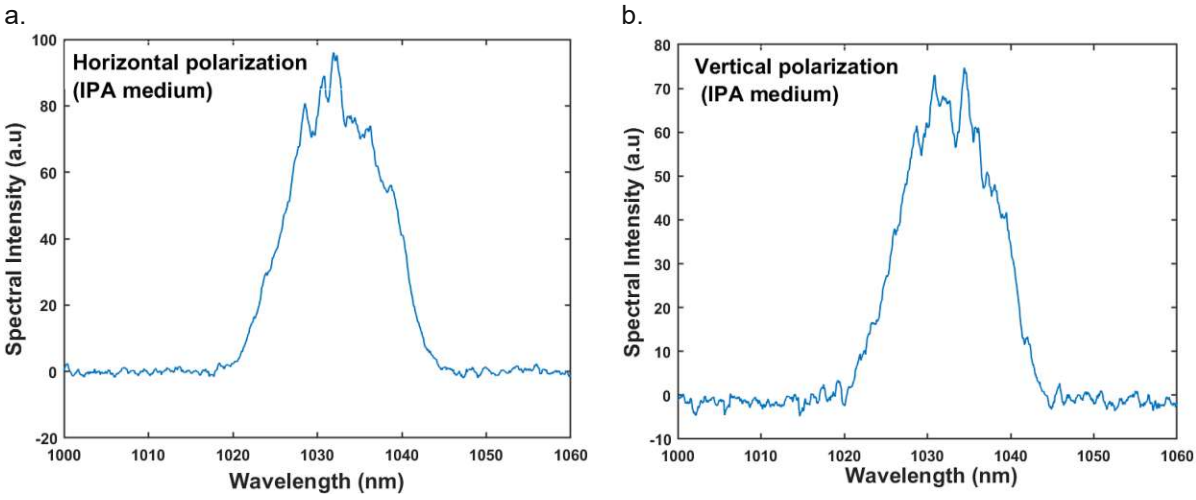

Figure 4.1. *Output spectra registered with input beam having a). horizontal polarization b). vertical polarization in the case of 20 cm length fiber in straight geometry with IPA in the external medium.*

It was observed experimentally that horizontally polarized optical light exhibited higher intensity compared to vertically polarized one as shown in ***Figure 4.1.***This implies that vertical polarization is prone to more losses due to the enhanced evanescent wave effect in the case of electric field vector oriented towards the thin glass region of the cladding.

Figure 4.2. shows the spectrum before and after immersing the sensing region into distilled water for both polarization orientation. The horizontal polarization results do not express any integral changes in the signal transmission, only the positions of the interference extremes were shifted after distilled water filling. In contrast, the vertical polarization results express also integral transmission changes with increasing character after filling of the tank.

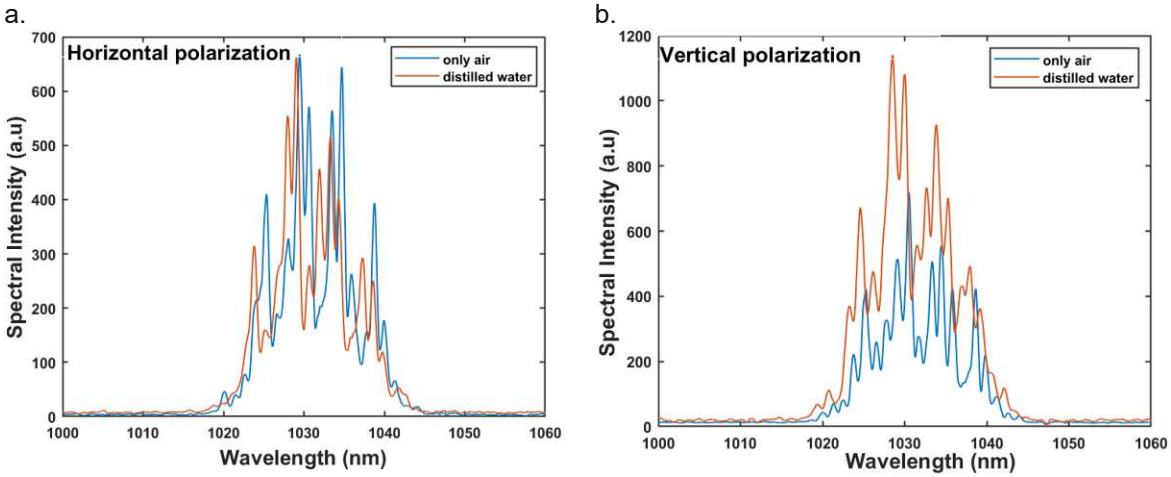

Figure 4.2. *Output spectra registered with input beam having a). horizontal polarization b). vertical polarization in case of 20 cm length fiber in straight geometry in case of air vs. distilled water as surrounding medium.*

These results indicate, the vertical polarization field is more advantageous for the liquid sensing application. ***Figure 4.2.*** expresses just moderate decrease of the transmission in case of vertical polarization, however the distilled water medium caused transmission improvement which exceeded both the levels (only air medium and distilled water medium) obtained at horizontal polarization. The registered change reveals the potential of the analyzed approach for liquid sensing and therefore it was further examined after realignment of the in-coupling and out-coupling geometry. The subsequent results confirmed the effect of transmission increase when applying liquid medium instead of air, both in the case of water and isopropanol (for both the polarization orientations).

In the case of water medium, the spectral intensity changes are moderate as shown in ***Figure 4.3b***. Whereas in ***Figure 4.3d***, it is observable that, isopropanol causes an increase of the transmitted spectral intensity up to one order of magnitude level. Similarly, to the outcomes of the water medium analysis, the vertical polarization of IPA medium expresses lower transmission and at the same time it has more pronounced changes comparing to the air.

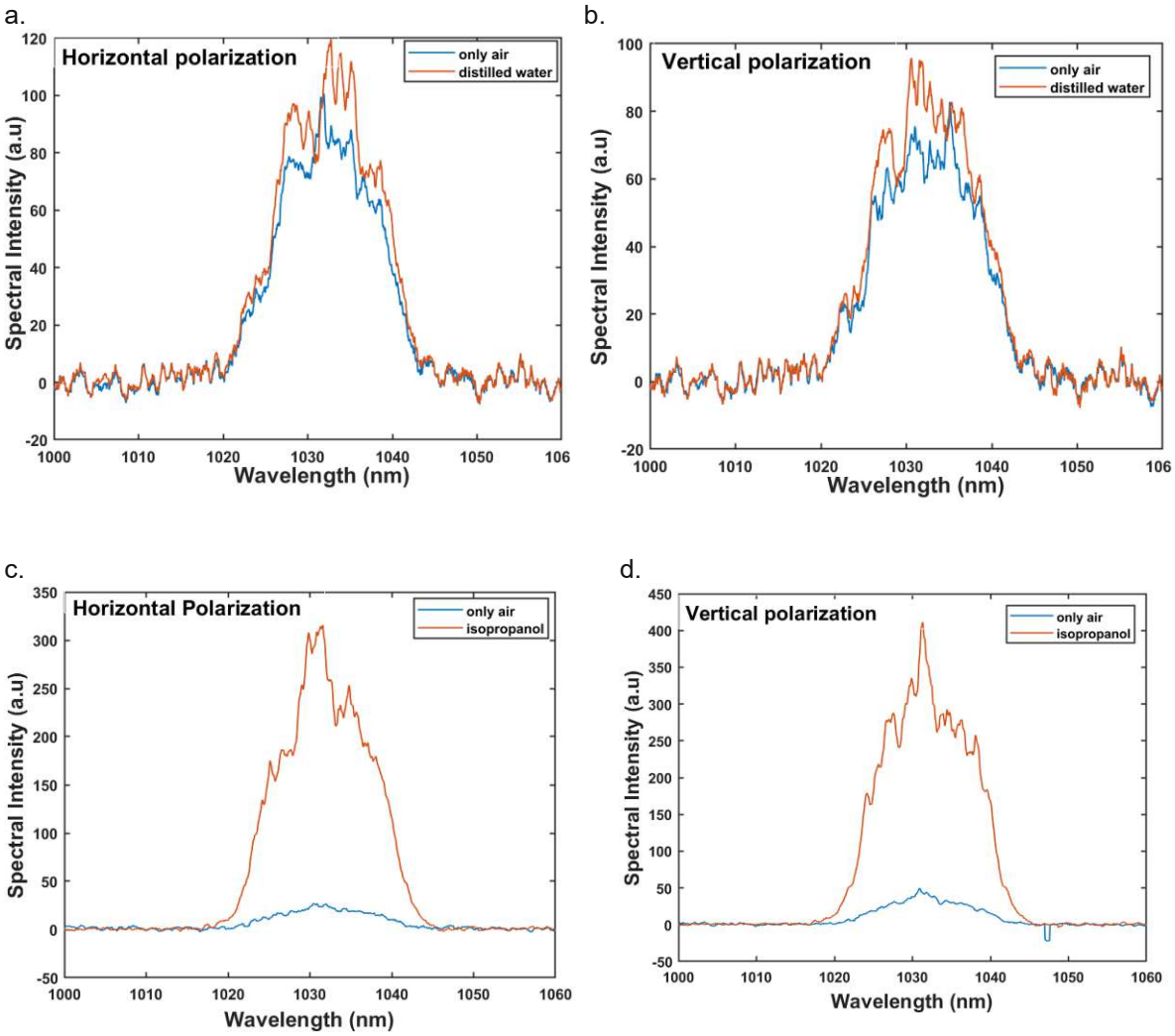

Figure 4.3. *Output spectra registered with input beam having a). horizontal polarization b). vertical polarization with distilled water and also with IPA having c). horizontal and d). vertical polarization in case of 20 cm length fiber in straight geometry.*

The next experimental investigation was devoted to IPA expressing higher transmission sensitivity. Under unchanged configuration the amount of the liquid was increased to subsequently fill the sensing region of the fiber in discrete steps. ***Figure 4.4.*** shows the spectral registrations results by increasing the length of the sensing region immersed into isopropanol with values 1 cm, 2 cm and 4 cm.

a. b.

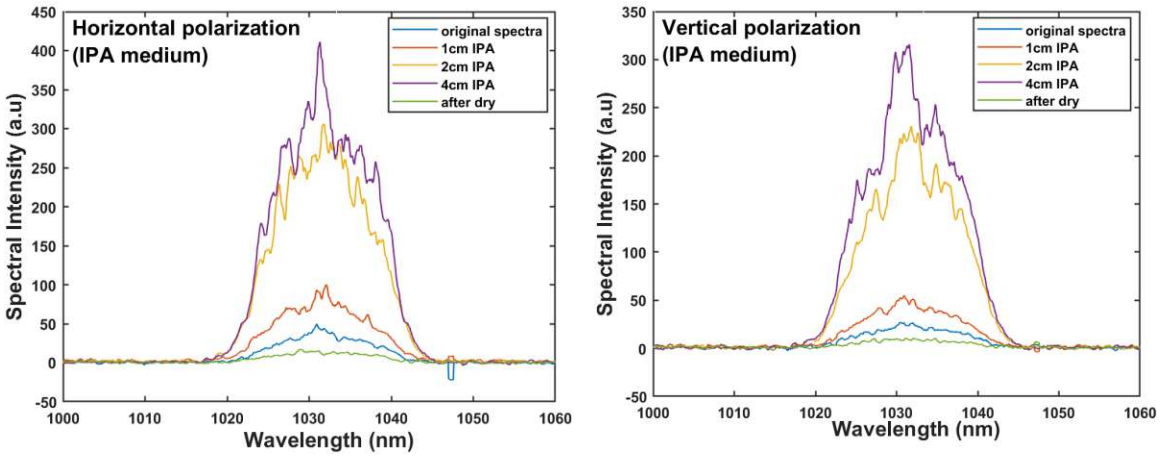

Figure 4.4. *Output spectra registered with input beam having a). horizontal polarization and b). vertical polarization in case of 20 cm length fiber in straight geometry in case of air vs. isopropanol as surrounding medium.*

The same behavior was observed as in the case of previous experiment focusing only on the spectral curves acquired from homogenous air vs IPA media: lower transmission and higher sensitivity on the surrounding media at vertical polarization. Moreover, the subsequent filling of the sensing volume resulted in monotonic increase of the transmission for the both polarization orientation. It is worth mentioning that in both the cases the removal of IPA and its complete evaporation brought again decrease of the transmission, however to lower level as the initial spectral registration in identical conditions. These observations invoke question about the reversibility of such sensing approach. The same behavior was observed registering the output radiation by the beam profiler camera exhibiting also monotonic increase of the intensity in the core region of the D-shaped fiber. The series of near field images in ***Figure 4.5.*** unveil the gradual change of the output beam shape and integral intensity increasing with the amount of liquid along the sensing region.

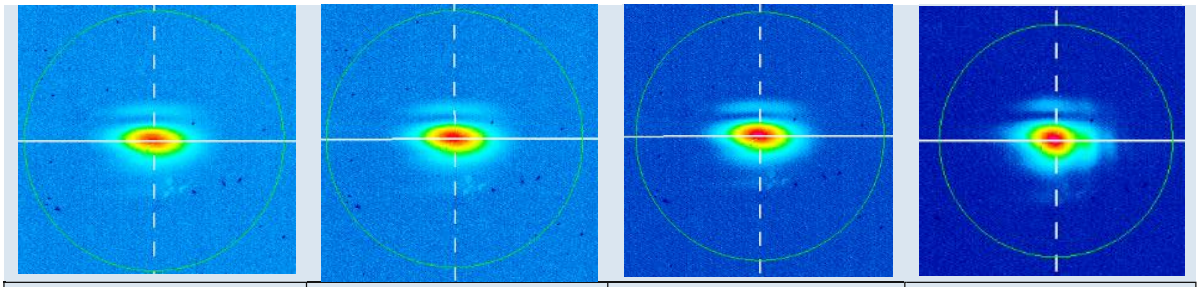

Only air	1cm IPA	2cm IPA	4cm IPA
Integration time 398.1 ms	Integration time 398.1 ms	Integration time 290.4ms	Integration time 225.4 ms

Figure 4.5 *Gradual change of the output beam shape and integral intensity increasing with the amount of liquid along the sensing region together with camera integration time.*

The image series expresses continuous change of the beam shape from elliptical towards spherical one and its effect was evaluated by calculating the ratio between the beam diameter in the two directions representing the orthogonal beam axis. The diameters towards the horizontal and vertical direction were acquired from the in-built image processing function of the beam profiler software as w_A and w_B respectively. The decrease of the ratio uncover the transition of the beam shape towards spherical one. ***Table 1*** presents the diameter values taken at the $1/e^2$ intensity level and their ratio.

Table 1. *The change of diameters towards horizontal and vertical directions depending on the increase in isopropanol amount along the sensing region.*

	Only air	1 cm IPA	2 cm IPA	4 cm IPA
w_A	1065 µm	1064 µm	1067 µm	835 µm
w_B	468 µm	479 µm	484 µm	484 µm
w_A/w_B	2.27	2.22	2.20	1.73
Ellipticity	0.44	0.45	0.45	0.58

The possible explanation of the increasing transmission in the case of IPA medium is the lower RI difference between the cladding and the medium comparing to water. The higher RI difference in the case of water causes similar behavior as in the case of air-glass interface. Due to the increasing transmission applying liquid medium around the fiber, elimination of the Rayleigh scattering losses is probable in the case of lower RI difference. The surface of the glass cladding has in general low optical quality especially after the uncoating process as seen in ***Figure 4.6.*** which can express increased amount of microcracks and residual acrylate particles. . The surface roughness is generally not important to be considered due to optical signal propagation only through the core. In case of D-shaped fiber, the flat surface of the cladding is near the core making it important to consider surface roughness caused by cladding material. The enhanced effect of the scattering in the case of higher RI difference causes enhanced losses of higher order modes modifying further the mode structure of the fiber. Whereas, in the case of scattering effect elimination due to better matching of the RI of the cladding, the original mode structure of the fiber is preserved better, which leads to increase in the throughput and makes the field distribution in the core more symmetrical.

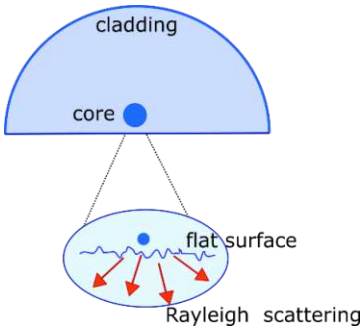

Figure 4.6. *The close localization of the uneven surface of the cladding to the fiber core can cause significant losses due to the evanescent wave effect.*

The intensity of the evanescent wave at the flat surface of the cladding is strongly dependent on the transversal mode under consideration. It is generally known, that the higher-order modes experience higher losses due to their higher intensity localization at the core-cladding interface [10] . The same is true in the case of the flat cladding surface, the distance of it from the fiber core is just 2 μm. In order to estimate the flat surface effect on the fiber mode structure, we calculated the number of guided modes in the D-shaped fiber. The number of modes can be calculated using the *V* parameter that is described in *section 2.2* applying conditions: wavelength of laser (λ =1030nm), core radius (a=7.55um), core refractive index (n_1=1.453), cladding refractive index (n_2=1.45)

$$\mathrm{V} = \frac{2\pi}{\lambda}\, a\sqrt{n_1^2 - n_2^2} = 4.27$$

Number of modes, $M \approx \frac{V^2}{2} = 9.36 \approx 9\ modes$

Figure 4.7a illustrates how the output beam shape is determined by guided modes ensemble when superposition principle takes place. The asymmetric character of the fiber cross section causes higher losses because among the same order modes in the fiber, some could have higher evanescent field effect than others. This could result in a spherically asymmetric beam shape. In principle, with increasing number of higher-order modes propagating in the fiber, there is increase of the evanescence wave effect beyond the fiber. Moreover, it has also a selective character in the case of the D-shaped fiber due to its spherical asymmetry. For example, the LP_{11b} mode has higher extent of evanescence field localized at the flat surface than the LP_{11a} mode as depicted in ***Figure 4.8***. The concept of the interpretation of the obtained results is that the lower RI difference eliminates the losses caused by the Rayleigh scattering on the flat surface due to the evanescent field. In order to have appropriateness of this concept, the reduction of the RI difference by applying IPA medium in the sensing region, should have two observable effects. Beside the output intensity increase it should be accompanied also with change of the beam shape from the elliptical towards the more spherical one.

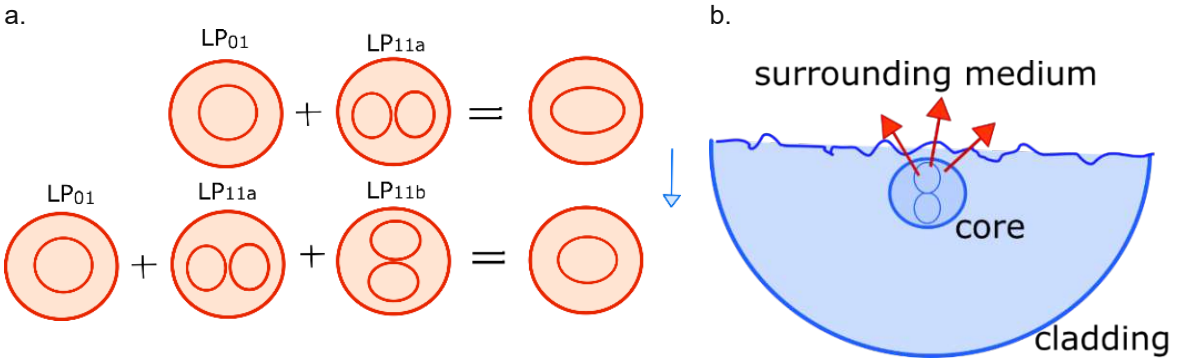

Figure 4.7. *a). Superposition effect of some lower- order modes in the case of asymmetric and symmetric propagation conditions b). The LP_{11b} mode is susceptible to higher losses due to the asymmetric character of the cross section.*

The above introduced concept is in correspondence with the output beam profile registration series presented in ***Figure 4.5.*** It confirms the monotonic change of the beam shape from elliptical to spherical character with increasing length of the sensing region merged into IPA. The final field distribution at completely merged sensing region should support the richest mode structure, therefore expresses the highest intensity and most spherical beam shape. It is important to stress that immersing the sensing region into water with higher RI difference does not cause such changes for either the intensity or in the beam shape.

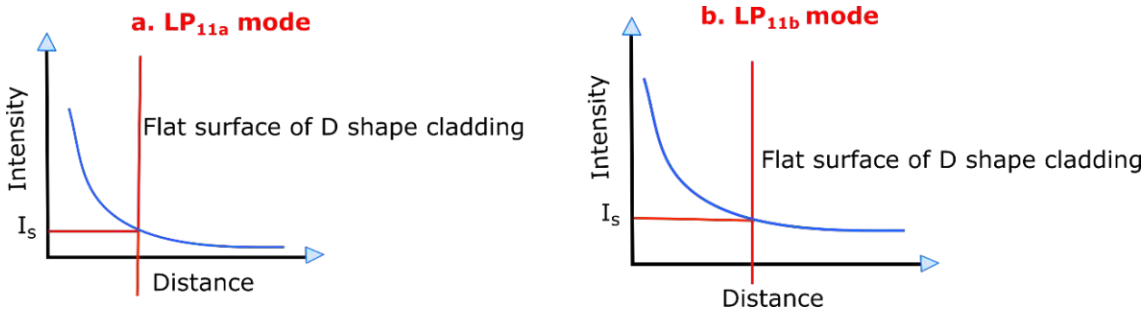

Figure 4.8. *Representative diagrams of higher order mode intensity reaching the fiber cladding flat surface with different orientation of its intensity extremes: a) LP_{11a} and b). LP_{11b}*

4.2 Water content in IPA solution

The observed significant difference between the water and isopropanol effect on the output field indicates a possibility of identification of water content in IPA- water mixture.

Isopropanol considered to be an industrially important chemical has various uses in applications like cosmetics, sanitizers and also in car care products. Contamination of isopropanol with water is hard to identify because they are nearly ideally miscible, distilled water is an odorless, tasteless liquid and the both media have negligible absorbance in region detectable by standard silica-based devices. Our sensing approach based on relatively simple fiber structure and registration devices provides a method to measure such contamination with notable precision.

A mixture of the two liquids were prepared with different measure of water content between values 100 µm and 900 µm volume in 1 ml solution. The distilled water proportion was increased sequentially with 100 µm steps, which resulted in 11 analytes including the pure IPA and water media. The experimental setup utilized fiber with length of 20 cm and 4 cm uncoated sensing region. The spectrum was registered for each mixture keeping the sensing region straight and completely immersed into the liquid. Spectral intensity enhancement was observed with increasing proportion of isopropanol in the sensing region. ***Figure 4.9.*** displays the IPA content dependence of the spectral intensity for both main polarization orientations. Vertical polarization experience higher losses and higher sensitivity on the property of the surrounding liquid medium in the case of this experiment. Moreover, the vertical polarization results exhibited monotonic dependence on the IPA content, while the horizontal polarization one experienced some discrepancy in the case of 6:4 volume ratio of the IPA-water mixture. It is another confirmation of the previously reported experiences that the vertical polarization should be preferred in the case of the suggested approach.

The measurements of optical signal took place in this experimental series using collection fiber of the spectrometer with 400 µm core diameter instead the previously used 200 µm core diameter one. It resulted in increase of the registered spectral intensity in the case of pure IPA and unveiled that the differentiation between the water and IPA transmission behavior is based in the integral intensity increase, without NA limitation effect in the case of the smaller diameter collection fiber. The higher absolute value of isopropanol shows that the spectral registrations have a memory effect that is accumulated from the previous spectral measurements and over time it shows higher absolute values of the spectrum. Also, pure distilled water spectral registration has a higher absolute intensity value when measured at the end of the experiment. This could have been due to deposits of some residues on the uncoated fiber region resulting from longer immersion time of sensing region in isopropanol. Hence, not all the sensing region was in direct contact with water causing discrepancy in the readings. Finally, the monotonic and

clearly distinguishable spectral curves in the case of measurement presented in ***Figure 4.9b*** indicates detection precision of the water contamination measure at least at the level of 5%. The results achieved are not with very high precision, but it is quite cheap technique that can be utilized for small scale measurements. A different geometrical configuration like U-bend can improve the precision to a more effective level.

a.

b.

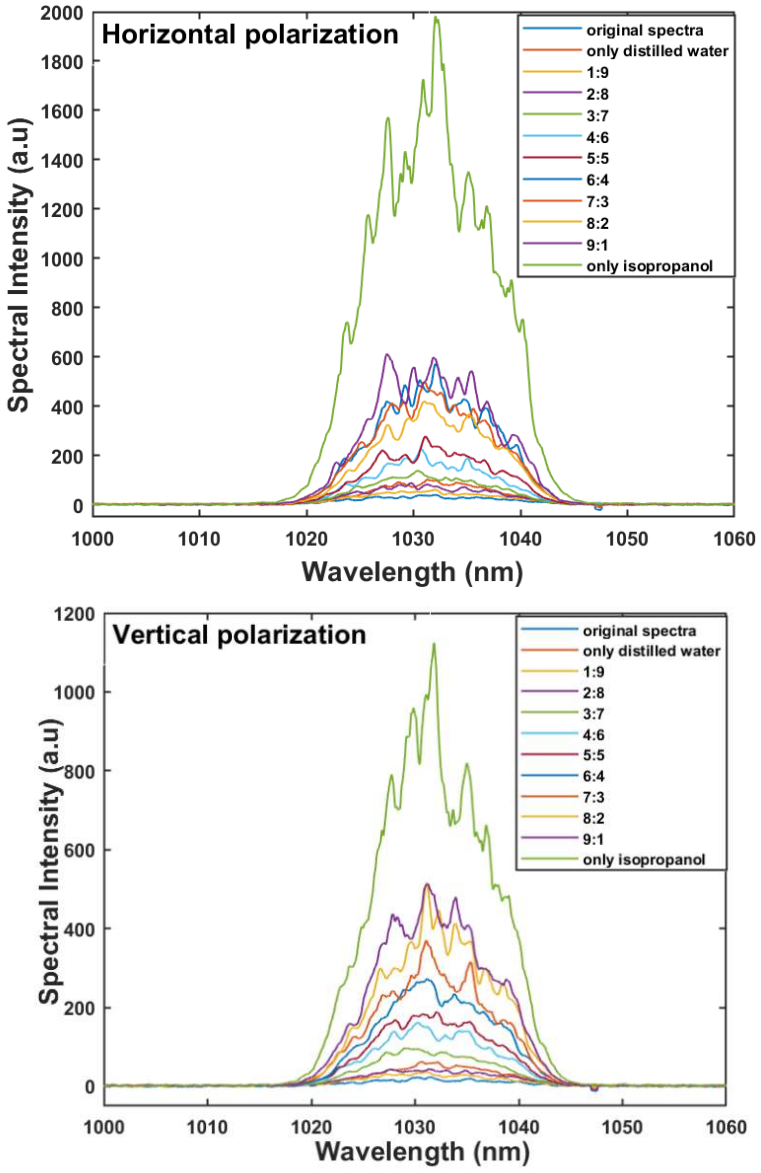

Figure 4.9. *D-shaped fiber transmission changes in mixture of isopropanol and distilled water with sequential change of their volume ratio for a). horizontal and b). vertical polarization.*

4.3 U-bend geometry

Other geometrical configuration was investigated as well to improve the fiber sensitivity based on evanescent wave-effect. The U-bend geometry is considered to be one of the useful approaches to enhance sensing performance. Another D-shaped fiber sample with 50 cm length was taken with 4 cm uncoated part in the central area, which acts as sensing region. The experimental setup was arranged to allow the sensing region of the fiber to be bend in the form of U and positioned in a tank which has the potential to contain liquid. Both liquids were tested and distilled water expressed again negligible changes of the output spectrum when the sensing region was completely immersed. Whereas, isopropanol exhibited extraordinary higher spectral intensity changes after the immersion process. The absolute values of intensity and the corresponding shifts were much higher than observed in straight geometrical configuration of the fiber.

The spectral registrations applying U-bend geometry are shown in ***Figure 4.10***. The important aspect of the U-bend geometry approach is the position of the core in relation of the direction of bending. However, due to the asymmetric character of the fiber cross section, the D-shaped fiber has the tendency to bend in geometry with core orientation inside the bending circumference. It is caused by the tension reduction effect during the bending process. The general theory of the U-bend effect on the mode propagation predict higher sensitivity effect in the case of the orientation at the outer circumference. By this way it is possible to enhance the evanescent wave absorption effect but our approach was focused more on the RI sensing.

According to the interpretation presented previously, the sensing effect is strongly connected to the measure of the higher-order mode losses. However, the losses effect is reduced when the core is oriented at the inner circumference due to larger angles of TIR, therefore the U-bend geometry support higher optical signal transmission and this feature was observed during this experimental series. According to our understanding the highest number of modes were transmitted exactly in this geometry. The transmission effect was again even more enhanced immersing the sensing region into IPA. The mutual benefit of evanescent wave effect elimination and index matching by the IPA media resulted in the highest spectral intensity enhancements presented in ***Figure 4.10.***

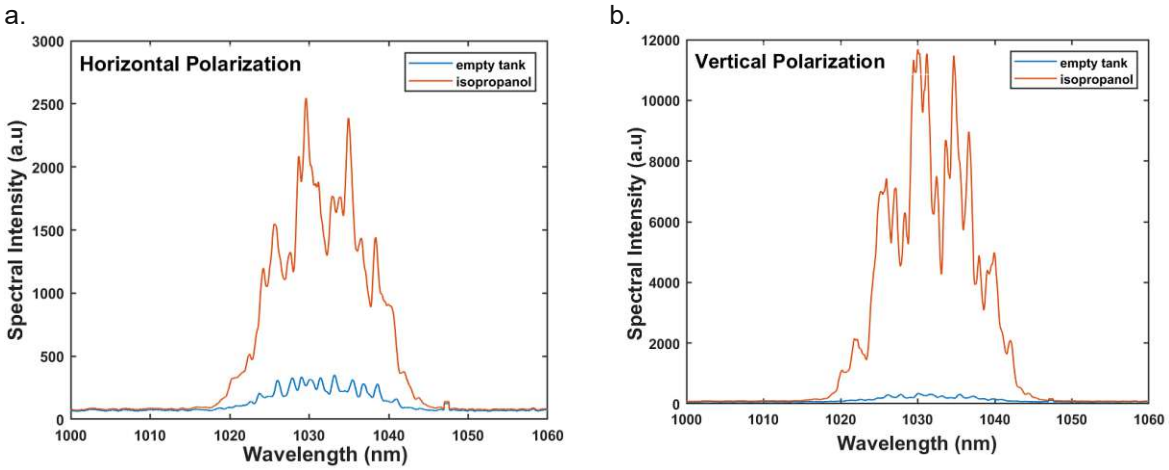

Figure 4.10. *Output spectra registered with input beam having a). horizontal polarization b). vertical polarization in case of 50 cm length fiber in U-bend geometry in case of isopropanol as surrounding medium.*

In order to compare the results obtained in different geometrical arrangements, the configuration of the experimental setup was fixed at the identical 50 cm fiber sample. Then measurements were performed in two cases, one before the formation of U-bend (straight geometry) another after the formation of U-bend. Finally, the ratios of the spectral intensities were constructed dividing the air medium values with the IPA medium ones.

The comparison of the results obtained in the case of straight and U-bend geometry for both the orthogonal polarization directions is presented in ***Figure 4.11.*** Spectral intensity ratios registered by the U-bend geometry at the vertical polarization of the input field displays the highest intensity changes acquired by this D-shaped fiber approach. This outcome also points out to the possibility of further enhancement of the detection precision of the water contamination in IPA, thus improving the application potential of the analyzed technique.

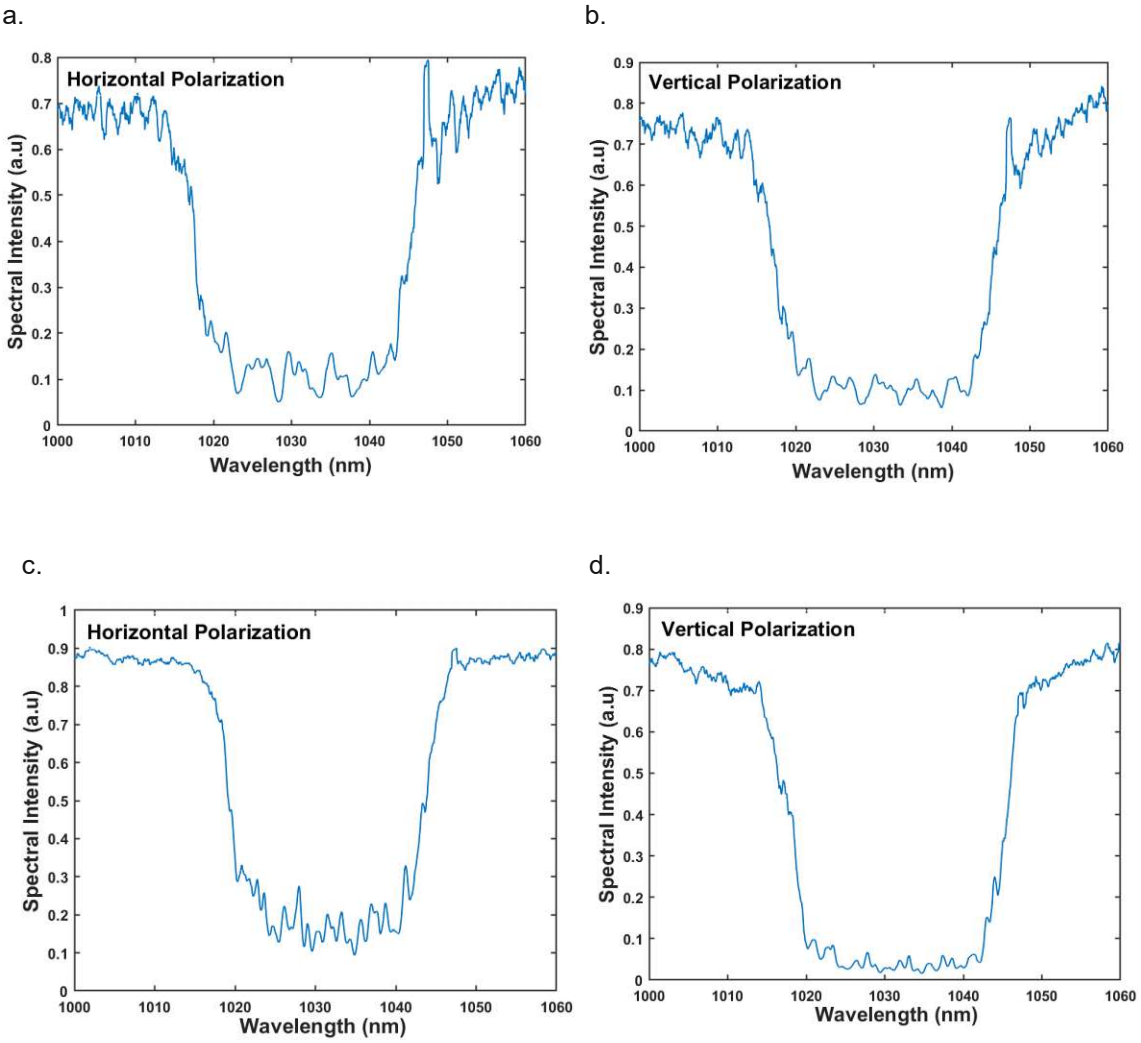

Figure 4.11. *Spectral intensity ratios for straight fiber geometry: ratio between the fiber in empty medium and in isopropanol for a). horizontal, b). vertical polarization and for U-bend geometry with c). horizontal and d). vertical polarization.*

5. CONCLUSIONS

The thesis focused on study of RI sensing performance based on evanescent wave effect. D-shaped fiber was investigated through the course of the thesis designed for applications of extrinsic sensing. One side of D-shaped being flat leads to high evanescent field localization in the external region beside the fiber. Such D-shaped fiber with length of 20 cm and 4 cm uncoated part serving as sensing region was utilized at the beginning. The uncoated part was situated in the middle of the fiber, which was arranged in straight geometrical configuration. Isopropyl alcohol and distilled water were the two liquids under test which were placed in the surrounding optical medium of the sensing region. Fiber based measurements exhibited simple design approach without any external power source required to activate the sensor system.

An interpretation of the outcomes was elaborated, based on the concept that the flat surface of the D-shaped fiber consists of small uneven surface which are prone to Rayleigh scattering. If the RI between the cladding and surrounding medium is less, the evanescent field experience reduced losses as in the case of isopropanol. Whereas for water, the difference in RI contrast is higher leading to scattering at the cladding surface, which eliminates the higher-order mode propagation via the evanescent field effect. Spectral and near field profile measurements were carried out to register the optical signal from the output end of the fiber. Distilled water proved to cause no changes regarding the spectral and spatial intensity. Whereas isopropanol medium exhibited significant difference in the transmitted intensities in comparison to the original spectrum recorded in air as surrounding medium. The sensitivity of the developed system was ensured according to our understanding due to reduced evanescent field based losses in the case of isopropanol.

Based on numerous spectral measurements performed in different conditions, an overview about the sensitivity of both the liquids were created. It helped to understand the water contamination in isopropanol, which is a widely utilized chemical material. Mixtures of isopropanol and water were prepared in different proportions and tested to verify the spectral changes observed with impure isopropanol. Contamination of isopropanol can be detected at least at the level of 5% precision of the water content. In addition to the results obtained, geometrical changes in the sensing region helped to improve the sensing performance. U-bend geometry was examined to enhance the sensitivity. Therefore, the thesis described a D-shaped fiber that can be used for RI sensing. The spectral increase in the transmission was an added advantage compared to the usual absorption

obtained with evanescent wave sensors. This helped to carry out measurements even with low signal level where detection of output signal became easier with increase in signal intensity in comparison to the case where absorption reduces the signal. Also, absorption can make detection of output signal harder if the initial signal level is low. Changes in the geometrical configurations e.g., to U-bend geometry improved the sensing effect. Thus, a novel chemical sensor approach was developed and tested using a specialty optical fiber with potential of further improvement of the sensitivity.

6. REFERENCES

[1] López-Higuera, J. M., Cobo, L. R., Incera, A. Q., & Cobo, A, ”Fiber optic sensors in structural,” *Journal of lightwave technology,* pp. 587-608, 2011.

[2] Bharadwaj, R., Sai, V. V. R., Thakare, K., Dhawangale, A., Kundu, T., Titus, S.... & Mukherji, S., ” Evanescent wave absorbance based fiber optic biosensor for label-free detection of E. coli at 280 nm wavelength,” *Biosensors and Bioelectronics,* pp. 3367-3370., 2011.

[3] Wren, S. P., Nguyen, T. H., Gascoine, P., Lacey, R., Sun, T., & Grattan, K. T., ”Preparation of novel optical fibre-based Cocaine sensors using a molecular imprinted polymer approach,” *Sensors and Actuators B: Chemical,* pp. 35-41, 2014.

[4] Sabri, N., Aljunid, S. A., Salim, M. S., & Fouad, S., ”Fiber optic sensors: short review and applications,” *Recent trends in physics of material science and technology,* pp. 299-311, 2015.

[5] Narayanaswamy, R., & Wolfbeis, O. S., ”Optical sensors: industrial, environmental and diagnostic applications,” 2004.

[6] Yu, H., Xiong, L., Chen, Z., Li, Q., Yi, X., Ding, Y., ... & Ding, Y., ”Ultracompact and high sensitive refractive index sensor based on Mach–Zehnder interferometer,” *Optics and Lasers in Engineering,* pp. 50-53, 2014.

[7] Gao, R., Jiang, Y., Ding, W., Wang, Z., & Liu, D., ”Filmed extrinsic Fabry–Perot interferometric sensors for the measurement of arbitrary refractive index of liquid.,” *Sensors and Actuators B: Chemical,* pp. 924-928.

[8] Shi, F., Wang, J., Zhang, Y., Xia, Y., & Zhao, L., ”Refractive index sensor based on S-tapered photonic crystal fiber.,” *IEEE Photonics Technology Letters,* pp. 344-347, 2015.

[9] Wu, Q., Chan, H. P., Yuan, J., Ma, Y., Yang, M., Semenova, Y., ... & Farrell, G, ”Enhanced refractive index sensor using a combination of a long period fiber grating and a small core singlemode fiber structure.,” *Measurement Science and Technology,* 2013.

[10] Liu, G., & Feng, D. , ”Evanescent wave analysis and experimental realization of refractive index sensor based on D-shaped plastic optical fiber,” *Optik,* pp. 690-693, 2016.

[11] Punjabi, N., Satija, J., & Mukherji, S., *In Sensing Technology: Current Status and Future Trends III, Springer, Cham,* pp. 25-45, 2015.

[12] Snyder, A. W. , ”Understanding monomode optical fibers,” *Proceedings of the IEEE,* pp. 6-13, 1981.

[13] Peacock, A. C., Gibson, U. J., & Ballato, J., ”Silicon optical fibres–past, present, and future.,” *Advances in Physics: X,* pp. 114-127, 2016.

[14] Jeffrey Cwalinski, P.E, ”Introduction to Fiber Optics,” Continuing Education and Development(ced)engineering.com.

[15] Igarashi, K., Souma, D., Tsuritani, T., & Morita, I. , ”Performance evaluation of selective mode conversion based on phase plates for a 10-mode fiber,” *Optics express.*

[16] ”Fosco Connect, Optical Fiber Loss and Attenuation,” [Online]. Available: https://www.fiberoptics4sale.com/blogs/archive-posts/95052294-optical-fiber-attenuation.

[17] ”Lasercalculator, Laser beam spot size calculator,” [Online]. Available: https://www.lasercalculator.com/laser-spot-size-calculator/.

[18] Maini, A. K., Lasers and optoelectronics: fundamentals, devices and applications, John Wiley & Sons., 2013.

[19] Massaroni, C., Saccomandi, P., & Schena, E., ”Medical smart textiles based on fiber optic technology: an overview.,” *Journal of functional biomaterials,* pp. 204-221, 2015.

[20] Liu, Z., Htein, L., Gunawardena, D. S., Chung, W. H., Lu, C., Lee, K. K., & Tam, H. Y. , ”Novel accelerometer realized by a polarization-maintaining photonic crystal fiber for railway monitoring applications,” *Optics express,* pp. 21597-21607, 2019.

[21] John, M. S., Kishen, A., Sing, L. C., & Asundi, A. , ”Determination of bacterial activity by use of an evanescent-wave fiber-optic sensor,” *Applied optics,* pp. 7334-7338.

[22] Shevchenko, Y., Camci-Unal, G., Cuttica, D. F., Dokmeci, M. R., Albert, J., & Khademhosseini, A., ”Surface plasmon resonance fiber sensor for real-time and label-free monitoring of cellular behavior,” *Biosensors and Bioelectronics,* pp. 359-367, 2014.

[23] Sharma, A. K., Gupta, J., & Sharma, I., ”Fiber optic evanescent wave absorption-based sensors: A detailed review of advancements in the last decade,” *Optik,* pp. 1008-1025, 2019.

[24] B. D. &. S. C. D. Gupta, ”Evanescent-absorption coefficient for diffuse source illumination: uniform-and tapered-fiber sensors.,” *Applied Optics,* pp. 2737-2742, 1994.

[25] Gupta, B. D., Tomar, A. K., & Sharma, A., ”A novel probe for an evanescent wave fibre optic absorption sensor,” *Optical and quantum electronics,* pp. 747-753, 1995.

[26] Wu, Y., Deng, X., Li, F., & Zhuang, X. , ”Less-mode optic fiber evanescent wave absorbing sensor: Parameter design for high sensitivity liquid detection,” *Sensors and Actuators B: Chemical,* pp. 127-133, 2007.

[27] Golnabi, H., Bahar, M., Razani, M., Abrishami, M., & Asadpour, A., ”Design and operation of an evanescent optical fiber sensor,” *Optics and lasers in engineering,* pp. 12-18, 2007.

[28] Xiong, Y., Zhu, D. Q., Duan, C. F., Wang, J. W., & Guan, Y. F. , ”Small-volume fiber-optic evanescent-wave absorption sensor for nitrite determination,” *Analytical and bioanalytical chemistry,* pp. 943-948, 2010.

[29] Wu, C. W., Chen, C. T., & Chiang, C. C., ”A novel U-shaped, packaged, and microchanneled optical fiber strain sensor based on macro-bending induced whispering gallery mode,” *Sensors and Actuators A: Physical,* pp. 86-91, 2019.

[30] Vijayan, A., Fuke, M., Hawaldar, R., Kulkarni, M., Amalnerkar, D., & Aiyer, R. C., ”Optical fibre based humidity sensor using Co-polyaniline clad.,” *Sensors and Actuators B: Chemical,* pp. 106-112, 2008.

[31] Yan, Q., Tao, S., & Toghiani, H., ”Optical fiber evanescent wave absorption spectrometry of nanocrystalline tin oxide thin films for selective hydrogen sensing in high temperature gas samples,” *Talanta,* pp. 953-961, 2009.

[32] Shukla, G. M., Punjabi, N., Kundu, T., & Mukherji, S., ”Optimization of plasmonic U-shaped optical fiber sensor for mercury ions detection using glucose capped silver nanoparticles.,” *IEEE Sesnors Journal,* pp. 3224-3231, 2019.

[33] Murugan, D., Bhatia, H., Sai, V. V. R., & Satija, J. , ” P-FAB: a fiber-optic biosensor device for rapid detection of COVID-19,” *Transactions of the Indian National Academy of Engineering,* pp. 211-215, 2020.

[34] Sai, V. V. R., Kundu, T., & Mukherji, S. , ”Novel U-bent fiber optic probe for localized surface plasmon resonance based biosensor,” *Biosensors and Bioelectronics,* pp. 2804-2809, 2009.

[35] Tan, A. J. Y., Ng, S. M., Stoddart, P. R., & Chua, H. S, ”Theoretical model and design considerations of U-shaped fiber optic sensors: A review,” *IEEE Sensors Journal,* pp. 14578-145589, 2020.

[36] Khijwania, S. K., & Gupta, B. D. , ”Maximum achievable sensitivity of the fiber optic evanescent field absorption sensor based on the U-shaped probe,” *Optics Communications,* pp. 135-137, 2000.

[37] Ruddy, V., MacCraith, B. D., & Murphy, J. A. , ”Evanescent wave absorption spectroscopy using multimode fibers.,” *Journal of Applied Physics,* pp. 6070-6074, 1990.

[38] Messica, A., Greenstein, A., & Katzir, A., ”Theory of fiber-optic, evanescent-wave spectroscopy and sensors,” *Applied optics,* Osa %1/%22274-2284, 1996.

[39] Snyder, A. W., Mitchell, D. J., & Pask, C. , ”Failure of geometric optics for analysis of circular optical fibers,” *JOSA,* pp. 608-614, 1974.

[40] Matias, I. R., Arregui, F. J., Corres, J. M., & Bravo, J., ”Evanescent field fiber-optic sensors for humidity monitoring based on nanocoatings,” *IEEE Sensors Journal,* pp. 89-95, 2006.

[41] Gravina, R., Testa, G., & Bernini, R., ”Perfluorinated plastic optical fiber tapers for evanescent wave sensing.,” *Sensors,* pp. 10423-10433, 2009.

[42] Krausz, F., Fermann, M. E., Brabec, T., Curley, P. F., Hofer, M., Ober, M. H., ... & Schmidt, A. J, ” Femtosecond solid-state lasers,” *IEEE Journal of Quantum Electronics,* pp. 2097-2122, 1992.

[43] Peterson, O. G., Tuccio, S. A., & Snavely, B. B., ”CW operation of an organic dye solution laser,” *Applied Optics Letters,* pp. 245-247, 1970.

[44] French, P. M. W., ”The generation of ultrashort laser pulses.,” *Reports on Progress in Physics,* 1995.

[45] Mahmoudi, P., Veladi, H., & Pakdel, F. G., ”Optogenetics, tools and applications in neurobiology,” *Journal of medical signals and sensors,* 2017.

[46] S. Poole, D. Payne, and M. Fermann, ”Fabrication of low-loss optical fibres containing rare-earth ions,” *Electronic Letters,* 1985.

[47] Mears, R. J., Reekie, L., Poole, S. B., & Payne, D., ” Neodymium-doped silica single-mode fiber lasers,” *Electroncis letters,* pp. 738-740, 1985.

[48] Liem, A., Limpert, T., Zellmer, H., Tunnermann, A., Reichel, V., Morl, K., ... & Harschak, A., ”1.3 kW Yb-doped fiber laser with excellent beam quality.,” tekijä: *In Conference on Lasers and ElectroOptics*, 2004.